Quarterly Report

Project Title:
Development of a Self-Sustained Wireless Integrated Structural Health Monitoring System for Highway Bridges

Cooperative Agreement # RITARS11HUMD

Fifth Quarterly Progress Report

Period:
July 15, 2012 through October 14, 2012

Submitted by:
The Research Team – University of Maryland with North Carolina State University and URS

Submitted to:
Mr. Caesar Singh, Program Manager, US DOT

Date: October 29, 2012

Table of Contents

EXECUTIVE SUMMARY

I — TECHNICAL STATUS

Accomplishments by Milestone

1.1. General

- Updated Project web site (http://www.ncrst.umd.edu/) (Task 1 and Deliverable 2)
- Delivered Fifth quarterly financial and technical reports (Task 6 and Deliverable 11)
- Working with NCDOT district engineers for Dr. Yuan's (NCST) testing NC bridges by wireless accelerometers.
- MD Bridge No. 1504200 I-270 over Middle brook Road, was first tested on March 19-21, 2012 and then second tested on June 28 &29, 2012. First test results were included in the Third and Forth quarterly report. Second test and continuously monitoring reports are included in this quarterly report. Sampling raw data of AE events and their corresponding strain gauges are shown in Appendix A and processed information with stress data by with Rainflow Counting Algorithm is shown in Appendix B.
- Real time strain and AE data monitoring is continuously viewed (, except two occasions due to thunderstorms and accidently pulled the plug by maintenance workers.) The following web address should display the BDI strain and AE data, both the graph and the properties.
  1) Try entering this web address into your browser (either Internet Explorer or Firefox should work fine)
  Link 1 to Remote BDI strain monitoring (link to http://166.143.163.215:8000/BDI.html)
  Link 2 to Remote AE sensor monitoring (link to http://166.143.163.215:8000/AE.html)
  2) It will then ask you to download the Labview plug-in, and direct you to the webpage with the download.
  3) After the plug-in is downloaded and installed, you should be able to view the file.

- The proposed work plan is shown below as Milestones/Deliverables. Dark Shading indicates Deliverable items and Tasks in which the Research Team has been engaged over the past quarters. Lighter shading indicates anticipated duration for Deliverables by quarters. Grid pattern shading means partially fulfilled.

Deliverables	Action	Quarter No.									
		1	2	3	4	5	6	7	8	9	10
1	Form TAC and conduct kick-off meeting. Determine baseline field test procedure (Task 1)										
2	Establish and update project web site (Tasks 1 & 6)										
3	Conduct baseline field test and finite element analysis on pre-selected bridges (Task 1)										
4	Design, fabricate and characterize AE sensor and measure the performance (Task 2)										
5	Develop and evaluate T-R method for passive damage interrogation (Task 3)										
6	Develop and experimentally evaluate wireless smart sensor and hybrid-mode energy harvester (Task 4)										
7	Implement passive damage interrogation T-R algorithm in the wireless smart sensor on bridges (Task 4)										
8	Integrate and validate AE sensors with wireless smart sensor and hybrid-mode energy harvester (Task 5)										
9	Develop and conduct field implementation/validation of commercial-ready ISHM system with remote sensing capability (Task 5)										
10	Recommend strategy to incorporate remote sensing and prognosis into BMS (Task 5)										
11	Prepare and submit quarterly status and progress reports and final project report (Task 6)										
12	Submit paper to conference presentations and publication to TRB meeting or other conferences (Task 6)										

Note: Deliverables items 7, 8 and 9 for the 5^{th} quarter are partially fulfilled. They are still tested and modified by the NCSU team. The explanation of the delay is described and highlighted on page 8 under Section 1.6 - Future Plan.

1.2. Remote Health Monitoring System

- Conditioned AirLink Raven Gateway for wireless networking and 3G connection
  - o Re-configured remote connection capabilities with the PXI
  - o Re-activated Gateway with static IP address
- Store data in a 5GB cloud drive from Amazon® to store data files
  - o Data files can be retrieved from our labs, with quick download times
  - o Maintain a Kill-A-Watt® to monitor power consumption of electrical devices
- Study the option using solar panel for sustainable system

1.3 Pilot Bridge Second Test and following activities

- MD Bridge No. 1504200 I-270 over Middlebrook Road testing was again performed on June 28-29, 2012, using deflection sensor for short term and AE and strain sensors for bridge long-term information collection. Stress range records were collected, which will be used as a reference for future testing. (Task 2 and Deliverables 4 & 9)
- Collected Weigh-in-Motion data from the Hyattstown southbound station, which is only few miles north of the bridge, as the input data to simulate the traffic on the bridge. Vehicle count report can be found from Internet Traffic Monitoring System operated by Maryland State Highway Administration. (Task 1 and Deliverables 1 & 3). Simulation process is shown in Appendix C.
- Conducted full test of the second pilot bridge field test – Full test was conducted and its FEM analyses of this pilot bridges were conducted. Appendix D shows the complete report of computer modeling for MD Bridge No. 1504200. (Task 2 and Deliverables 4 & 9)

1.4 AE Sensor

- Long-term remote acoustic emission monitoring of the existing fatigue cracks has been carried out on the I-270 Middlebrook Bridge near Germantown, Maryland since July 10, 2012. Meaningful AE data that suggests the existing fatigue crack (as shown in Figure 1) is active and may be further propagating was collected from long term monitoring. Close examination of these three signals shown in Figure 1(b) reveals that some phase shift occurs between the signals, suggesting this AE event must be induced by near-field source. Figure 2 shows the average frequency spectra of the triggered AE signals of these three piezoelectric film AE sensors. 92 AE signals similar to those shown in Figure 2(b) were used for this averaging. It is seen that there is an attenuation of 8 dB from Channel #1 signal to Channel #2 signal. Considering this attenuation relationship reflected in the measured AE signals, it is believed that the AE signals were triggered by AE activities associated with fatigue crack.

- Conducted testing on piezo film AE sensor on four full-scale tube specimens in the lab - piezo paint AE sensor with new pattern to maximize frequency shift caused by fatigue crack growth are currently being tested in the steel welded tube specimens in lab, as shown in Figure 3. Piezo paint based AE sensors are installed on the steel tube specimens as shown in Figure 4 and 5. Seven piezo film AE sensors are installed on each specimen to monitor any AE signal caused by fatigue crack initiation and propagation. So far we have tested four specimens and the average fatigue life is found to be 600k cycles under a stress range of 22 ksi, which is comparable to the stress level observed on the connection plate of the field test bridge in Maryland.

- Testing and validating piezo film AE sensor in the lab with more extensive tests to characterize its performance including steel plates of different thickness that are commonly seen on bridge structures. Benchtop test involving glass capillary breakage and pencil break were conducted to characterize the broadband performance of piezo film AE sensors as well as the attenuation effect of plastic substrate layer on AE signals. Further experimental test of a frequency shift based crack source location algorithm and Rayleigh wave attenuation relationship based crack source localization method were conducted using both the field test data and the AE data collected from the steel tube fatigue test. This near-field AE monitoring strategy is being refined for piezo film AE sensor and has the advantage of improved representation of crack source information. It was also found that flexible piezo paint AE sensor worked well on curved steel tube specimens while PZT discs broke when bonding the sensor to the tube surface. A Labview-based portable AE monitoring system is also currently tested on the steel tube fatigue test specimens.

(a)

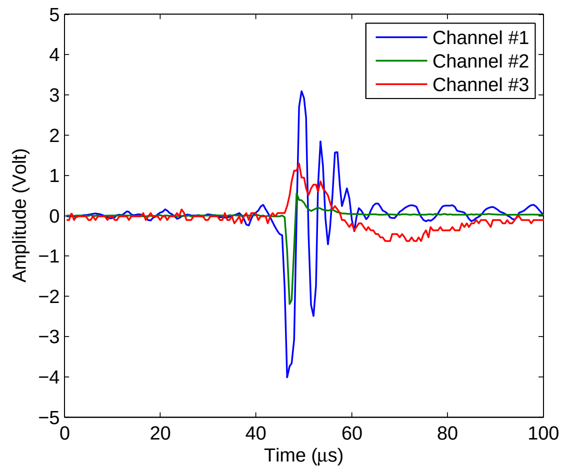

(b)

Figure1 - (a) Three piezoelectric film AE sensor near fatigue crack tip on the connection plate; (b) Typical AE signal measured by the three piezoelectric AE sensors.

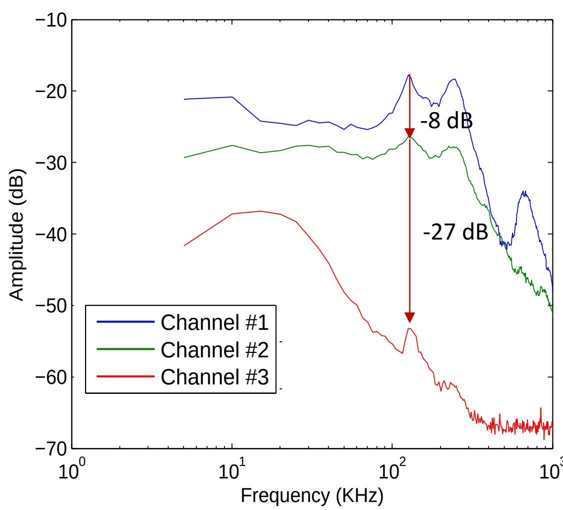

Figure 2 - Average frequency spectrum of triggered AE signals by three piezoelectric film AE sensors.

Figure 3 - test setup for fatigue testing of full-scale steel tube from traffic signal post

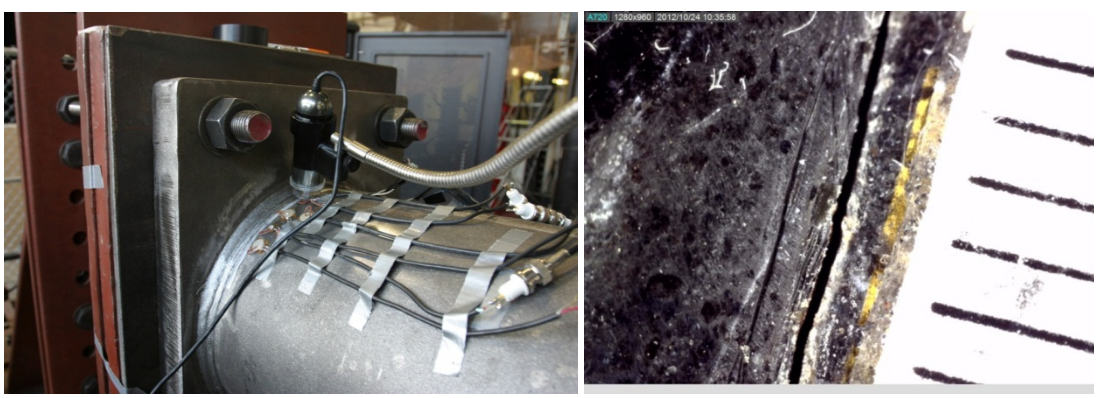

Figure 4. Digital microscope used for measuring fatigue crack size and growth (left) and pictures of fatigue crack taken using digital microscope (magnification x50)

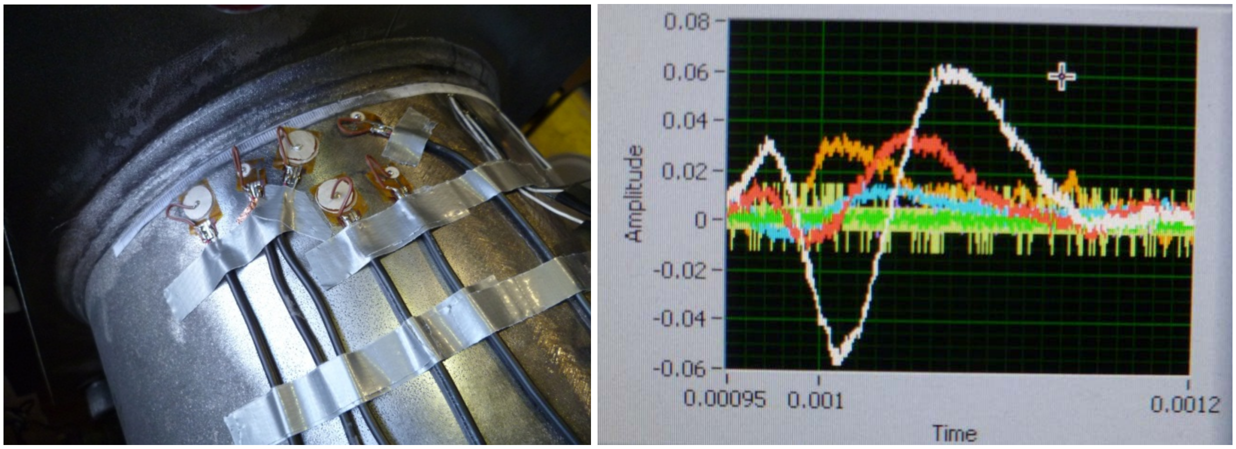

Figure 5. Piezo film AE sensor (left) and AE signals triggered by fatigue crack growth

Figure 6. Picture of a large piezo paint patch (size about 2 x 5 inches) made in our lab for sensor fabrication

1.5 T-R Method, Energy Harvesting and Smart Sensor

Accomplishments of these tasks by NCSU team are detailed in Appendix E and summarized here:

- The performance of the wireless accelerometer sensor has been tested successfully in the laboratory. The wireless sensor was mounted on a shaker where a sine excitation 15Hz was excited. Then the PSD of the acceleration data collected by the sensor was calculated and compared with the excitation frequency. Test results demonstrated that the wireless sensor functioned well in the lab).
- Performance tests of the whole wireless sensor networks (WSN) has also been carried out (Five wireless accelerometer sensors were installed on a small bridge in Lake Raleigh to simulate a short duration of WSN for collecting acceleration information of the bridge. Calculating the PSD of acceleration data collected by all sensors under different scenarios, then we plotted the first two mode shapes of the bridge by using the calculated PSD results. The tests result demonstrated that the WSN also functioned well for a short time monitoring).
- An energy harvesting system has been installed on Beaufort #25 Bridge with the assistance from North Carolina DOT (At present, the installation of solar panel has been completed and the miniature wind turbines are being fabricated and will be installed shortly).
- The base station has been manufactured and installed (See details in the deployment part).

- A finite element model of Beaufort #25 Bridge has been established (the modal analysis has been carried out, which was used to compare with the test data. However, the FE model needs to be further examined in details for accurately reflecting the test results).

1.6 Future Plans

Pilot Bridge Testing (UMD team led by Dr. Fu) –

- There will be another on-the-bridge test scheduled for Nov. 15 & 16, 2012 to conduct full test to validate all measured data.
- Continue monitoring, evaluating and validating results from the 2nd pilot testing bridge (MD Bridge No. 1504200 I-270 over Middlebrook Road)
- Long-term monitoring using AE sensors on the pilot test bridge in Maryland
- Preparing field testing T-R method, energy harvesting and smart sensors on the pilot test bridge in NC
- Collecting more W-I-M data to simulate more traffic through FEM models for all pilot test bridges in Maryland and NC
- Validating test data with FEM results for the cause of fatigue.

AE Sensor (UMD team led by Dr. Zhang) -

- Continue the long-term fatigue crack growth monitoring with piezo film AE sensor and remote sensing features on I-270 bridge in Maryland. On site test including other instruments and integration test with NCSU participation is planned for November 15 and 16, 2012. In the next quarter, AE signals will be collected from this system and analyzed for possible fatigue crack growth associated with the existing fatigue cracking on the bridge. Integrating wireless transmitter with piezo paint AE sensor will be examined during the field test. Data analysis of the field monitoring data from remote sensing system will be conducted including synchronization of sensors with different modality (such as BDI strain gages and piezo film AE sensors of different sampling rate) will be conducted.
- Continue the testing of AE sensor on two additional full scale tube specimens in the lab - piezo paint AE sensor with new pattern to maximize frequency shift caused by fatigue crack growth will be tested in the steel welded tube specimens in lab. The next quarter will involve characterizing these AE sensors with integrated wireless sensing feature. Two piezo film AE sensors integrated with wireless sensor board will be installed on the specimen to monitor any AE signal caused by fatigue crack initiation and propagation.

T-R Method, Energy Harvesting and Smart Sensor (NCSU team led by Dr. Yuan) -

- The program used to support reliable communication between PC to base station and sensors needs to be enhanced until it can steadily work for a long-term monitoring (we have tested the whole WSN for a short-term monitoring, but it is unstable for a long-term stability. There are some bugs in the hardware of the original board and the program when the whole WSN works for extended time. **Therefore more time is needed, perhaps, to redesign the sensor board and debug this whole program absolutely, maybe these will continue for several months to come**).
- Installing the WSN and other accessories on the bridge.

II — BUSINESS STATUS

- Hours/Effort Expended – As the last reporting period, PI Dr. Fu worked one month paid by his cost sharing account for 167 man-hours. Three (3) UM and two (2) NCSU graduate assistants worked three months half-time (20 hours), the quarterly accounting deadline, for a total of 1,470 man-hours (one NCSU assistant is partially cost-shared by their University.)
- Hours/Effort spent by the NC State for in-kind cost share ($130,000) is counted for here..
- Funds Expended and Cost Share –
    - Listed and invoiced in this Quarterly Federal Financial Report (period ending on Sept 30, 2012): Federal share of expenditure requested for this quarter $72,876.04 [Federal share total $389,168.12; Recipient share of expenditure (cost share) $395,430.04, which is shown in an excel file; Cumulative Total $784,598.16]
    - $130,000 in-kind cost sharing contribution by NCDOT on equipment, personnel, consultation, and road-side assistance on the bridge test is included.

Appendix A – AE events and their correspondence with strain gauges

Appendix B – Applied Rainflow Counting Algorithm with Stress Data

Appendix C - Traffic Loading Simulation

Appendix D – Global and Local Models for the crack locations of the Maryland Pilot Bridge

Appendix E – NCST Report for NC Beaufort County Bridge

Appendix A – AE events and their correspondence with strain gauges

By Tim Saad and Chung C. Fu

Four sets of sampled AE events (peaks) with their corresponding stresses are shown here. Data were collected remotely and these sampled results are dated 7/14/12 and 7/15/12. The first chart of the 4 chart set in the following figures portrays the time history of stress data for one-hour of data. The AE event that occurred during this time is portrayed with a green dot. The second chart provides a more detailed (zoomed-in) view of the stress data, with the AE event portrayed with a green dot at the time of its occurrence. The last chart shows the voltage data from the AE event which was previously depicted by the green dot.

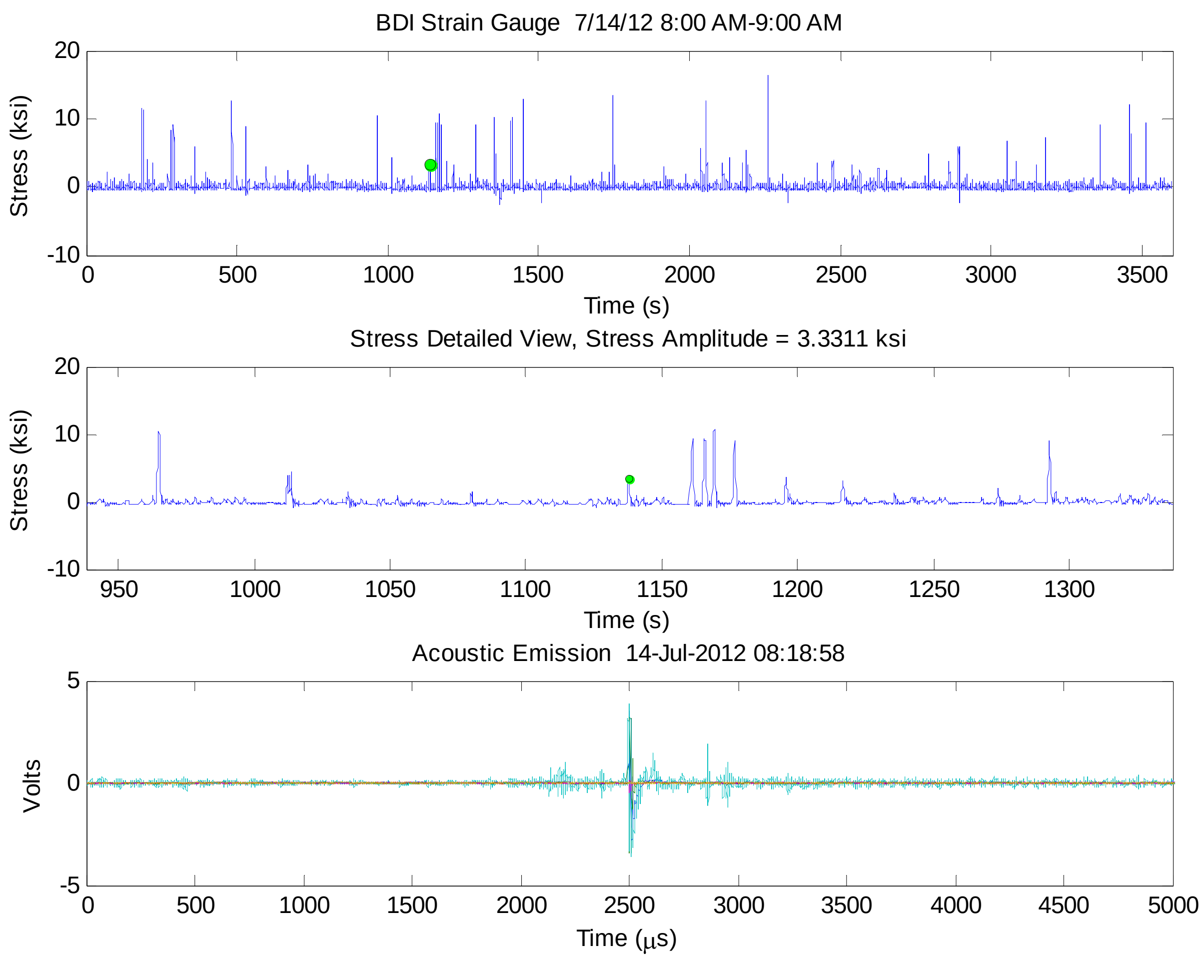

Figure 1 – Data 8-9 am 7/14/12 (a) Stress within one-hour period, (b) zoom-in data and (c) AE event

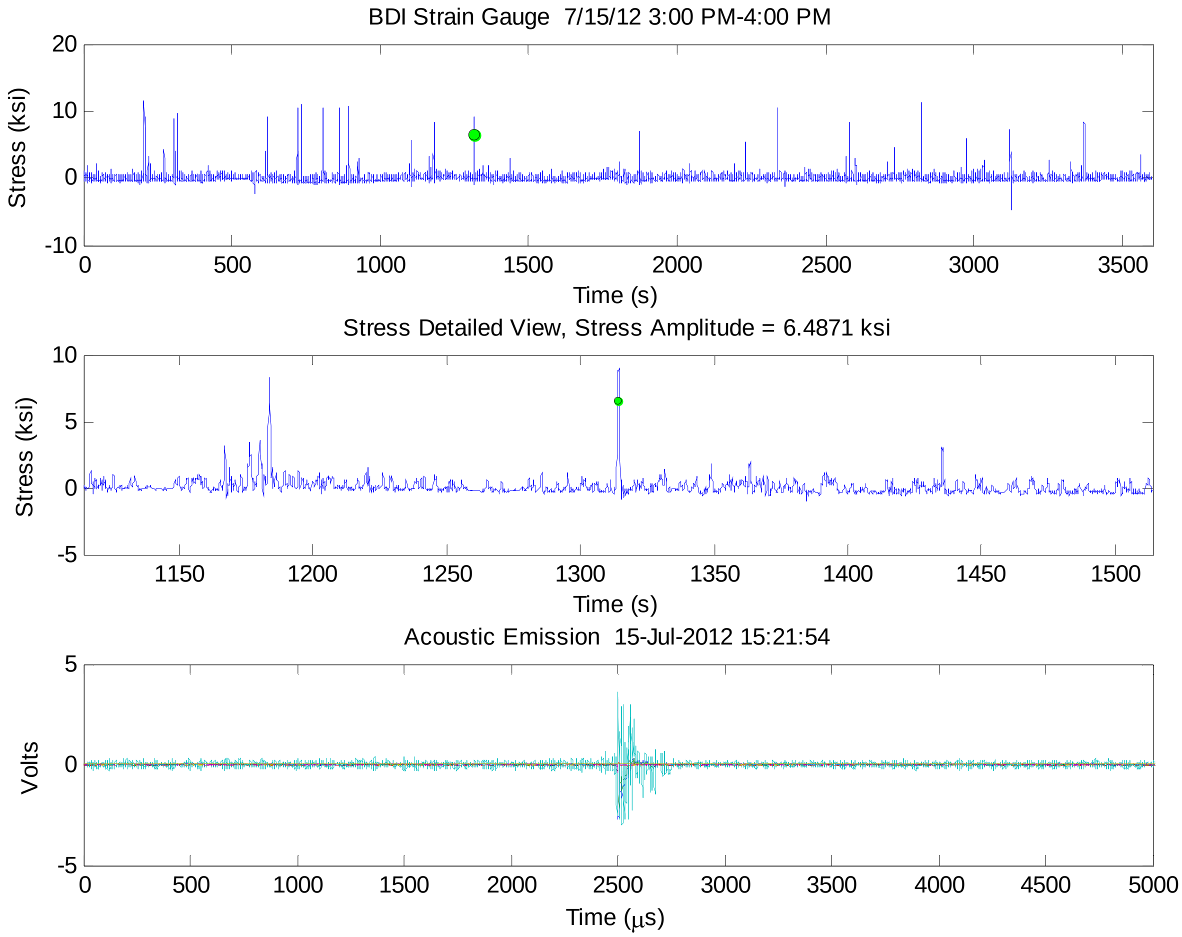

Figure 2 – Data 3-4 pm 7/15/12 (a) Stress within one-hour period, (b) zoom-in data and (c) AE event

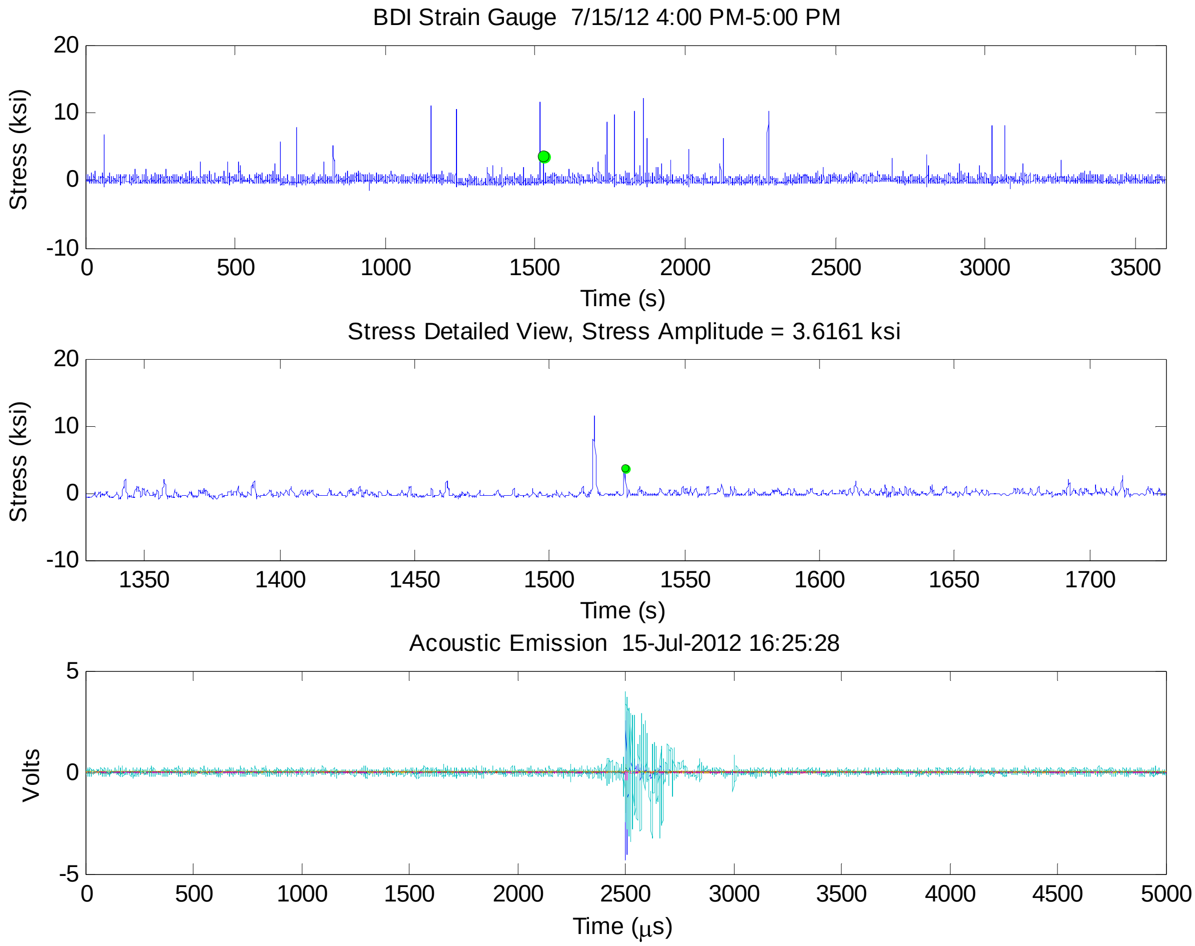

Figure 3 – Data A 4-5 am 7/15/12 (a) Stress within one-hour period, (b) zoom-in data and (c) AE event

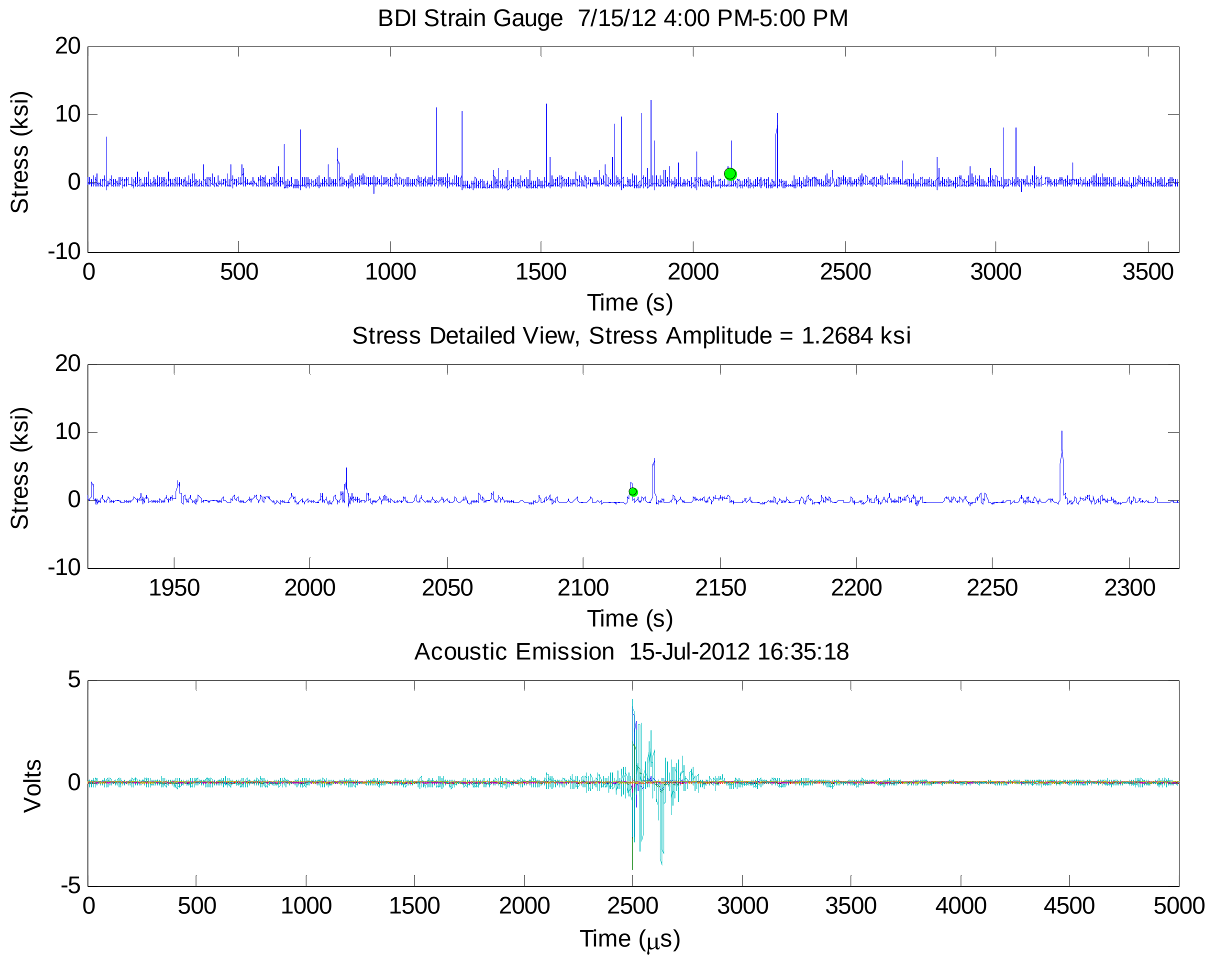

Figure 4 – Data B 4-5 pm 7/15/12 (a) Stress within one-hour period, (b) zoom-in data and (c) AE event

Appendix B – Applied Rainflow Counting Algorithm with Stress Data

By Tim Saad and Chung C. Fu

Rainflow counting algorithms are used to extract cycles from a load history. Each of these cycles is associated with closed stress-strain hysteresis loops, which are associated with the energy dissipation the fatigue damage.

The figures shown below illustrate the applied rainflow cycle counting algorithm to four hours of acquired stress data on July 11, 2012. The rainflow matrix (bottom left) provides illustration in 3D view for the number of counted cycles with their given amplitudes and their corresponding mean values from the 1-hour of stress history.

The histogram in the bottom right illustrates in 2D view the distribution of mean values of rainflow cycles (on the x-axis) vs. the number of cycles on the y-axis.

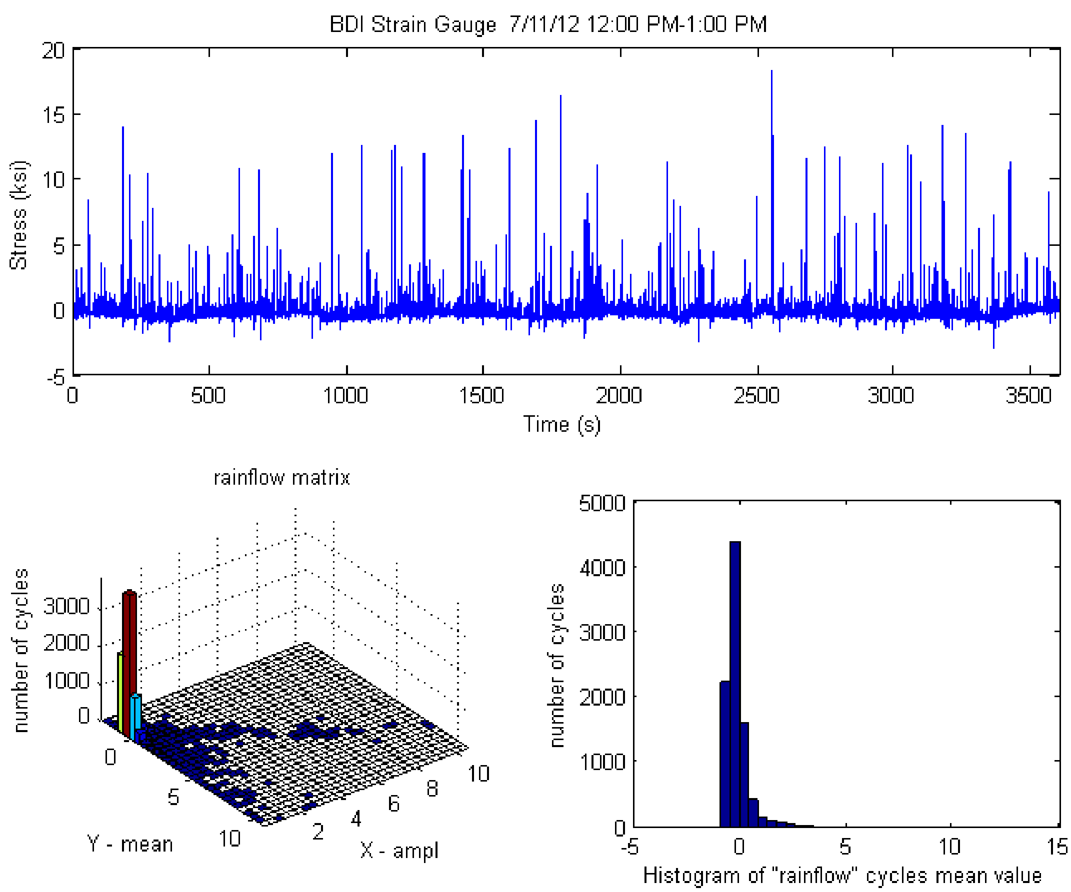

Figure 1 – Data 12-1 pm 7/11/12 (a) Strain data (b) 3D view - no of cycles with amplitudes and mean values (c) 2D view - no of cycles with mean values

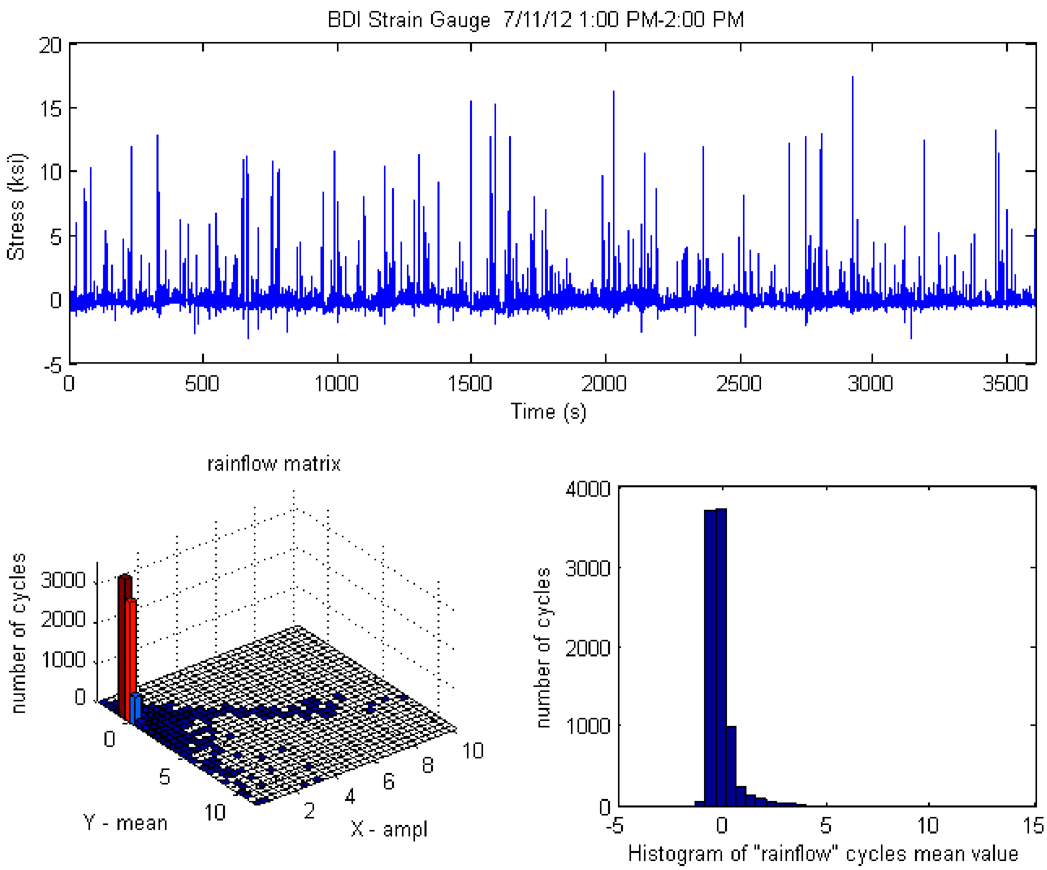

Figure 2 – Data 1-2 pm 7/11/12 (a) Strain data (b) 3D view - no of cycles with amplitudes and mean values (c) 2D view - no of cycles with mean values

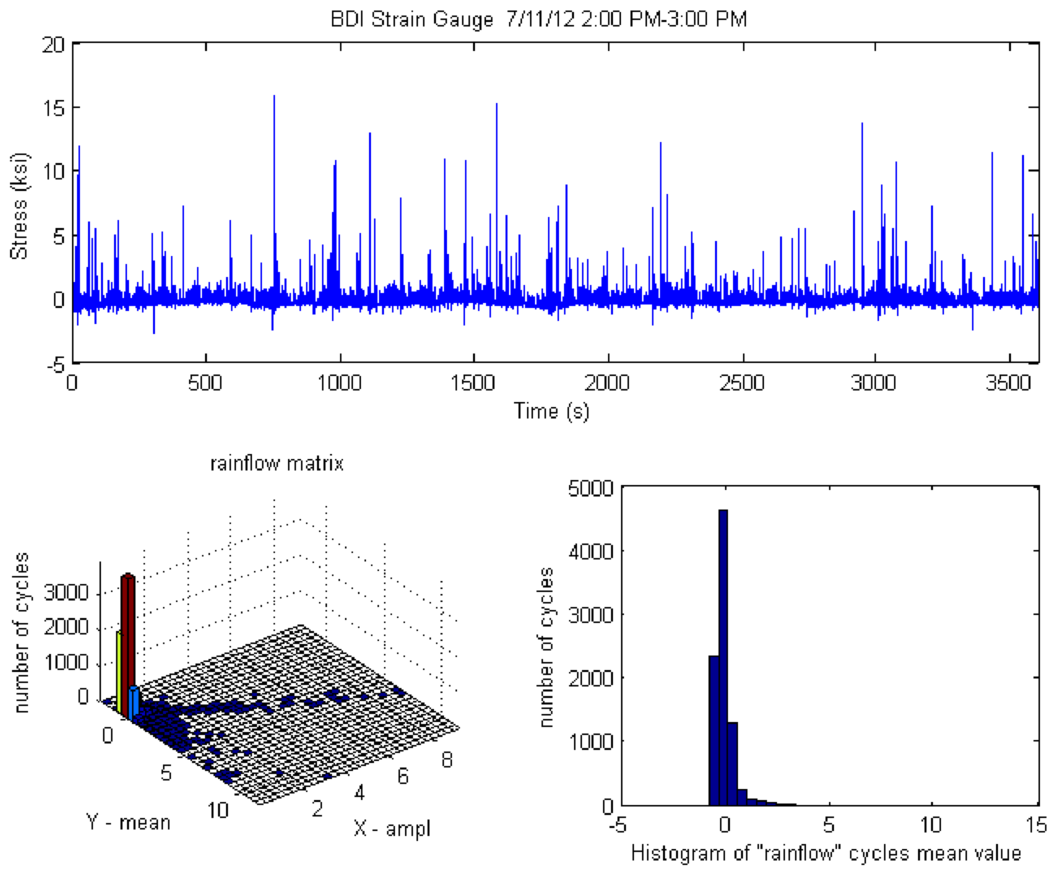

Figure 3 – Data 2-3 pm 7/11/12 (a) Strain data (b) 3D view - no of cycles with amplitudes and mean values (c) 2D view - no of cycles with mean values

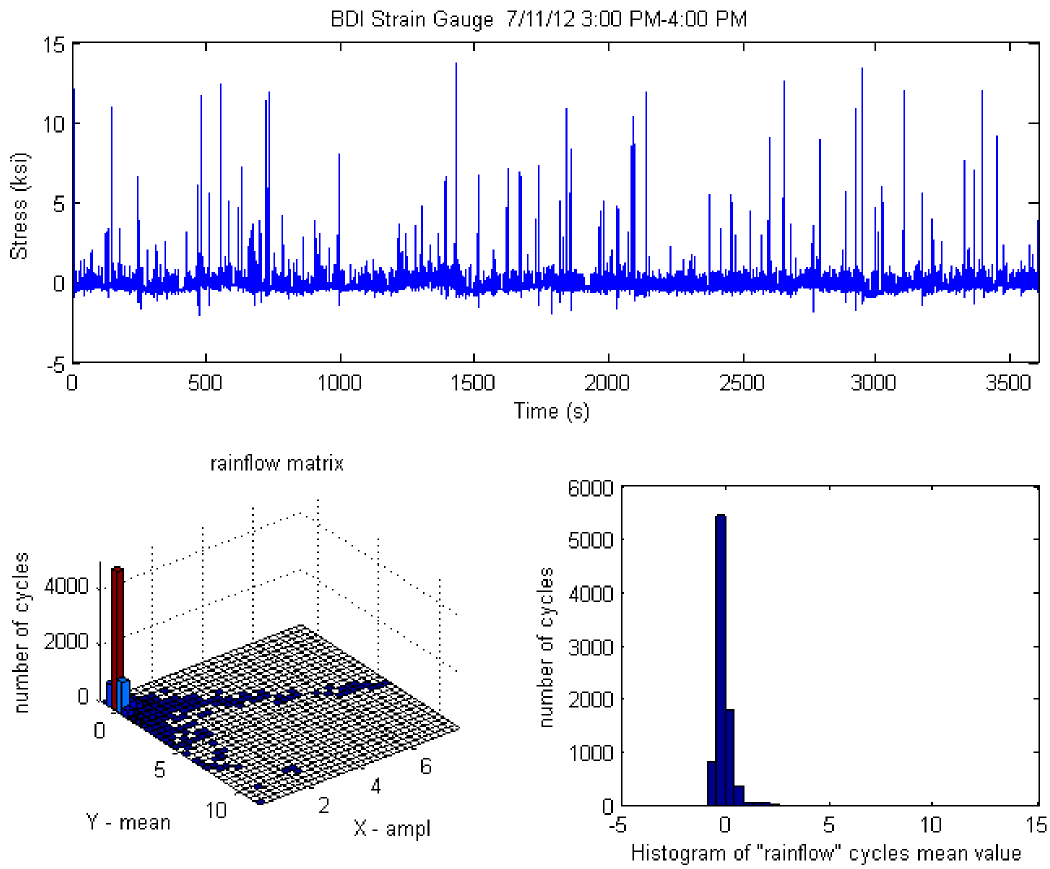

Figure 4 – Data 3-4 pm 7/11/12 (a) Strain data (b) 3D view - no of cycles with amplitudes and mean values (c) 2D view - no of cycles with mean values

Appendix C - Traffic Loading Simulation

By Gengwen Zhao and Chung C. Fu

1. Introduction

CORSIM is a comprehensive microscopic traffic simulation, applicable to surface streets, freeways, and integrated networks with a complete selection of control devices (i.e., stop/yield sign, traffic signals, and ramp metering). It simulates traffic and traffic control systems using commonly accepted vehicle and driver behavior models. CORSIM combines two of the most widely used traffic simulation models, NETSIM for surface streets, and FRESIM for freeways. It has been applied by thousands of practitioners and researchers worldwide over the past 30 years and embodies a wealth of experience and maturity. It is adopted here to simulate the bridge traffic.

2. Simulation procedure

(1) Build the simulation network in TSIS 5.1 around the MD Bridge No. 1504200 I-270 over Middlebrook Road based on the background map obtained from Google Map. The background map is adjusted to the correct scale and the simulation network is drawn along the real roadway segment. The network contained the mainline of I270 and adjacent on-ramps of the bridge in the studies. Since we only focus on the southbound of the bridge, the network only contains one-way southbound link. The simulation time is set to be one hour.

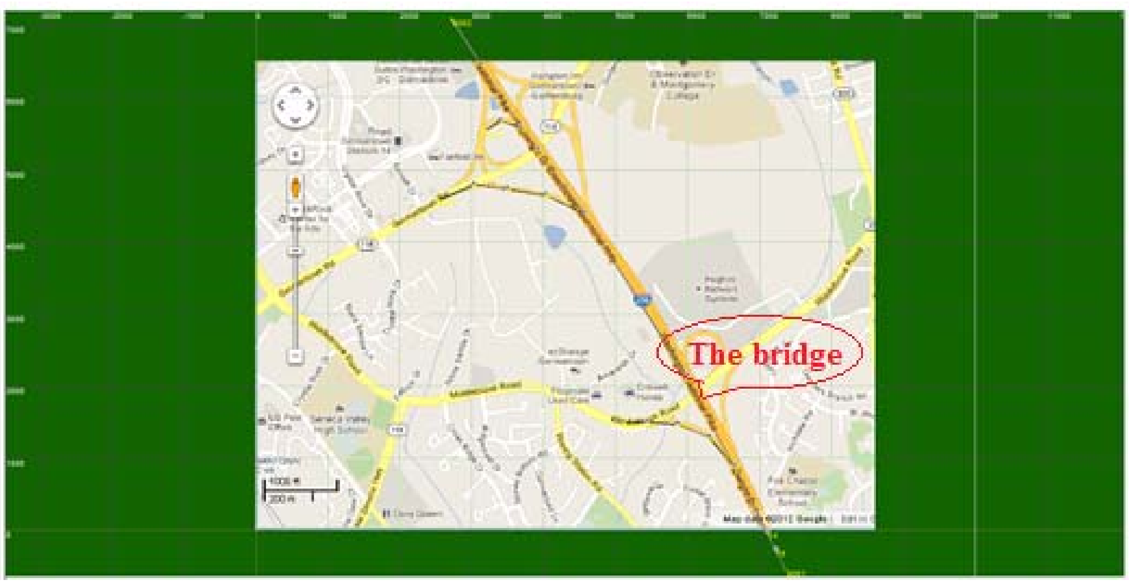

Figure 1 Simulation network

(2) Use the time varying vehicle count data collected from nearby detectors and combine with the Weigh-in-Motion data collected from the Hyattstown southbound station as the input data for the simulation model. Vehicle count report can be found from Internet Traffic Monitoring System operated by Maryland Department of Transportation State Highway Administration. (http://shagbhisdadt.mdot.state.md.us/ITMS_Public/default.aspx)

The truck count data is converted to truck percentage (truck count/ total vehicle count) as the input for CORSIM simulation. The truck percentage for the study site is around 4%.

Maryland Department of Transportation
State Highway Administration
Highway Information Services Division

Vehicle Occupancy Count Report

Station ID : S1997150044 **Count NO :** 665239
Location : IS 270 SOUTH OF MD 118 **Complied By :** General User
Date : 06/06/2007
Comments: This is a combined file

Lane 8 S **Occupants**

Beginning Hour	1	2	3	4	>= 5	Van Pool	Bus	Truck	Total
06:00	304	30	6	0	0	0	5	13	345
06:15	371	40	1	2	0	0	1	15	415
06:30	352	44	1	0	0	0	5	13	402
06:45	399	40	3	0	0	0	3	4	445
07:00	384	38	3	1	0	0	2	5	428
07:15	352	26	4	0	0	1	4	5	387
07:30	389	24	1	0	0	0	0	10	414
07:45	383	23	4	2	0	0	2	8	414
08:00	400	36	0	0	0	2	4	8	442
08:15	393	28	2	0	0	0	2	6	425
08:30	366	23	1	0	0	0	4	6	394
08:45	315	29	2	0	0	1	2	8	349
09:00	290	17	0	1	0	0	4	13	312
09:15	266	22	0	0	0	0	2	6	290
09:30	230	14	0	0	0	1	4	8	249
09:45	190	13	1	0	0	0	7	7	211
Total:	**5384**	**447**	**29**	**6**	**0**	**5**	**51**	**135**	**6057**
S Total:	**25427**	**1,945.00**	**87.00**	**37.00**	**2.00**	**58.00**	**157.00**	**1,114.00**	**28827**
Grand Total:	**42470**	**4,975.00**	**250.00**	**87.00**	**12.00**	**108.00**	**316.00**	**1,608.00**	**49,826.00**

Figure 2 Part of Vehicle Count Report from SHA

1	ID	TIME	GROSS	CLASS	FLAGS	SPEED	AXLES	A01WT	A01SPC	A01FLG	A02WT	A02SPC	A02FLG	A03WT	A03SPC	A03FLG	A04WT	A04SPC	A04FLG	A05WT	A
2	675115421	10/1/2009 12:31	54100	9	524290	61.9091	5	9950	12.3	0	11960	4.3	0	12070	35.9	0	9930	4.1	0	10160	
3	604510055	10/1/2009 12:31	8800	5	1024	48.2727	2	4310	12.6	0	4520	0	0	0	0	0	0	0	0	0	
4	671990812	10/1/2009 12:49	35900	9	0	62.4545	5	11610	15.7	0	6640	4.5	0	6750	34.3	0	5130	4.1	0	5790	
5	671947059	10/1/2009 13:11	17500	5	1024	48.4773	2	7390	21.3	0	10060	0	0	0	0	0	0	0	0	0	
6	545274165	10/1/2009 13:15	76200	2	1024	52.8409	2	800	8.7	0	1110	0	0	0	0	0	0	0	0	0	
7	671780125	10/1/2009 13:16	69500	9	0	54.2045	5	11110	15	0	16390	4.4	0	15440	35.5	0	12980	4.1	0	13560	
8	671695418	10/1/2009 13:31	21000	6	0	58.7727	3	11930	18.5	0	4880	4.3	0	4200	0	0	0	0	0	0	
9	604521219	10/1/2009 13:33	34800	8	0	51.9545	4	10600	13.4	0	11650	32.4	0	6530	4.1	0	6020	0	0	0	
10	604398020	10/1/2009 13:38	43000	9	0	50.5909	5	10840	14.6	0	8630	4.4	0	8700	33.7	0	7150	4.1	0	7680	
11	671945749	10/1/2009 13:38	65600	9	1024	52.7727	5	11160	11.6	0	15630	4.4	0	15240	35	0	11620	4.1	0	11980	
12	671779317	10/1/2009 13:59	77200	9	0	62.25	5	10730	15.7	0	16760	4.3	0	17060	32.4	0	15810	4.1	0	16800	
13	672007708	10/1/2009 14:14	63400	9	0	58.1591	5	10980	11.8	0	13850	4.3	0	14870	36	0	11590	4.1	0	12150	
14	671705390	10/1/2009 14:20	61200	11	0	58.0227	5	11420	17.5	0	16050	21.9	0	14070	9.2	0	9930	22.7	0	9730	
15	671689068	10/1/2009 14:35	77400	9	573440	57.8182	5	11440	16.9	0	15210	4.3	0	15740	34.7	0	17370	4.1	320	17640	
16	546035960	10/1/2009 14:59	74000	9	0	54.6818	5	10420	19.5	0	16670	4.3	0	16960	30.9	0	14990	10.2	0	14960	
17	671990033	10/1/2009 15:30	81800	9	577536	52.5	5	11850	16.9	0	17090	4.4	320	17260	33.7	320	18460	4.1	320	17100	
18	672002259	10/1/2009 15:31	52100	9	0	51.3409	5	11290	17.3	0	11640	4.3	0	11620	30.8	0	9300	4.1	0	8270	
19	671680932	10/1/2009 15:37	75900	9	0	58.4318	5	11280	16.9	0	15630	4.3	0	16310	35.2	0	15020	4.1	0	17670	
20	671989983	10/1/2009 16:02	37000	9	1024	54.0682	5	12340	15.7	0	7170	4.4	0	6920	34.1	0	5030	4.1	0	5560	
21	545710711	10/1/2009 16:10	48400	9	0	52.2955	5	10910	16.1	0	9470	4.3	0	9620	32.6	0	8990	4.1	0	9420	
22	604525839	10/1/2009 16:13	36800	9	1024	49.1591	5	11030	16.4	0	6930	4.4	0	6590	13.4	0	6240	4.1	0	6010	
23	604523658	10/1/2009 16:24	64000	9	0	59.4545	5	9720	17.7	0	12490	4.3	0	11800	36.1	0	14820	4.2	0	15180	
24	671780191	10/1/2009 16:24	71200	9	1024	58.3636	5	11310	15.6	0	16360	4.3	0	16430	35.6	0	11870	4.1	0	15230	
25	671723644	10/1/2009 16:34	79200	9	0	49.9091	5	11680	19	0	15370	4.4	0	14280	28	0	18400	10.2	0	19430	
26	671774176	10/1/2009 16:36	53200	9	0	50.7955	5	11970	17.1	0	13640	4.4	0	13590	32.1	0	7020	4.1	0	7020	
27	604390417	10/1/2009 16:49	51700	9	0	62.3182	5	10350	19.7	0	9940	4.4	0	10180	32.9	0	10430	4.1	0	10770	

Figure 3 Part of the Weigh-In-Motion Data

(3) Install three loop detectors at the bridge in the created simulation network, one for each lane in order to record the speed, type and passage time of the detected vehicles.

(4) Simulation result

After the simulation network was completely created, the traffic demand was input and calibrated, and the detectors were installed, the CORSIM simulation could be started. The simulation could provide the following meaning results for the analysis. First, it records the animation of the simulation which is used to observe the passage time of the trucks as shown in Figure 4. Second, it provides text output including the volume and speed statistics by each interval (set to be 1s here) as shown in Figure 5. Combining the above two output, the passage time and the lane occurred and speed of the truck could be successfully matched.

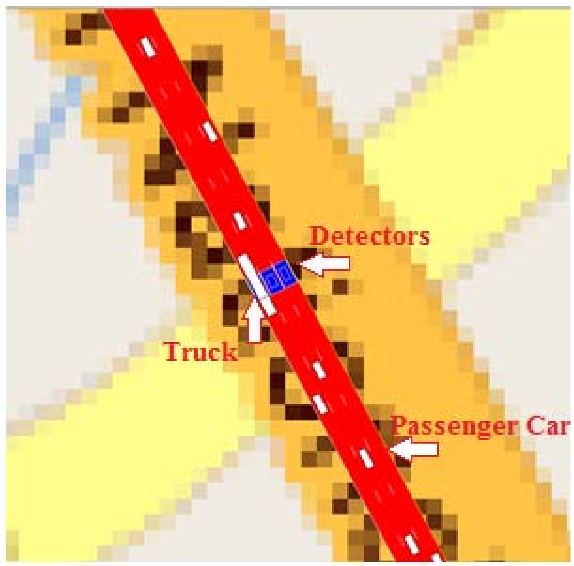

Figure 4. Animation Result

POINT PROCESSING OUTPUT

EVALUATION PERIOD BEGINNING TIME = 8 (SECONDS)
EVALUATION PERIOD ENDING TIME = 8 (SECONDS)
NEGATIVE VALUE MEANS NO INFORMATION

LINK	LANE ID NO.	DISTANCE FROM UPST. NODE (FT)	LOOP LENGTH (FT)	STATION NO.	DETECTOR TYPE	VOLUME (VPH)	MEAN SPEED (MPH)	MEAN HEADWAY (SEC)	MEAN OCCUPANCY RATE
(4, 5)	1	247.00	20.0	1	SINGLE SHORT LOOP	3600	55.887	1.225	23.050
(4, 5)	2	247.00	20.0	2	SINGLE SHORT LOOP	3600	-1.000	-1.000	0.000
(4, 5)	3	247.00	20.0	3	SINGLE SHORT LOOP	3600	53.060	2.995	25.700

1

Figure 5. Part of the Detector Output

3. Traffic loading pattern

Select continuous 10 minutes traffic flow from the one hour simulation results as the traffic loading pattern for finite element model.

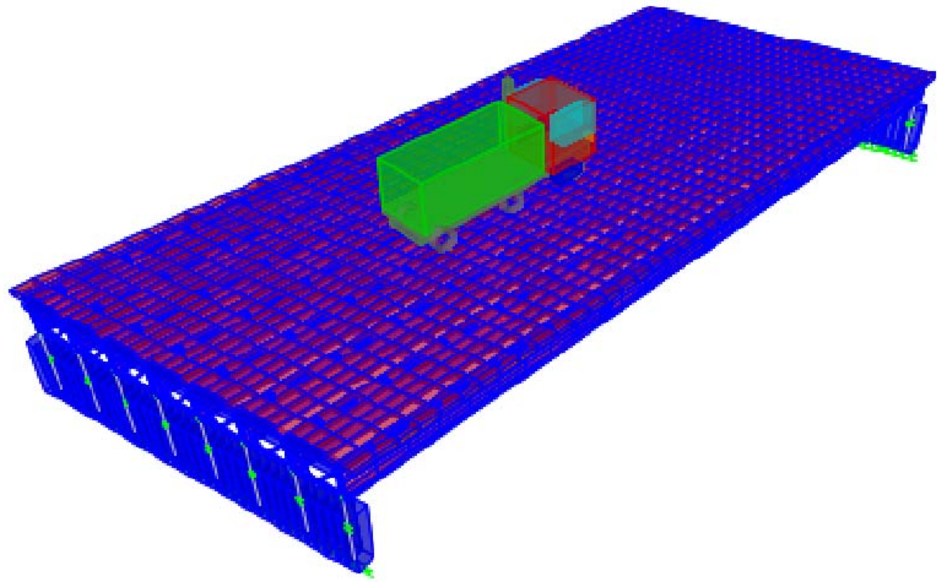

Figure 6. Bridge under Traffic Loading

Appendix D – Global and Local Models for the crack locations of the Maryland Pilot Bridge

By

Chung C. Fu, Gengwen Zhao and Tigist Getaneh

Instrumentation plan is shown in Figure 1 – Crack locations and sensor placement on the framing plan.

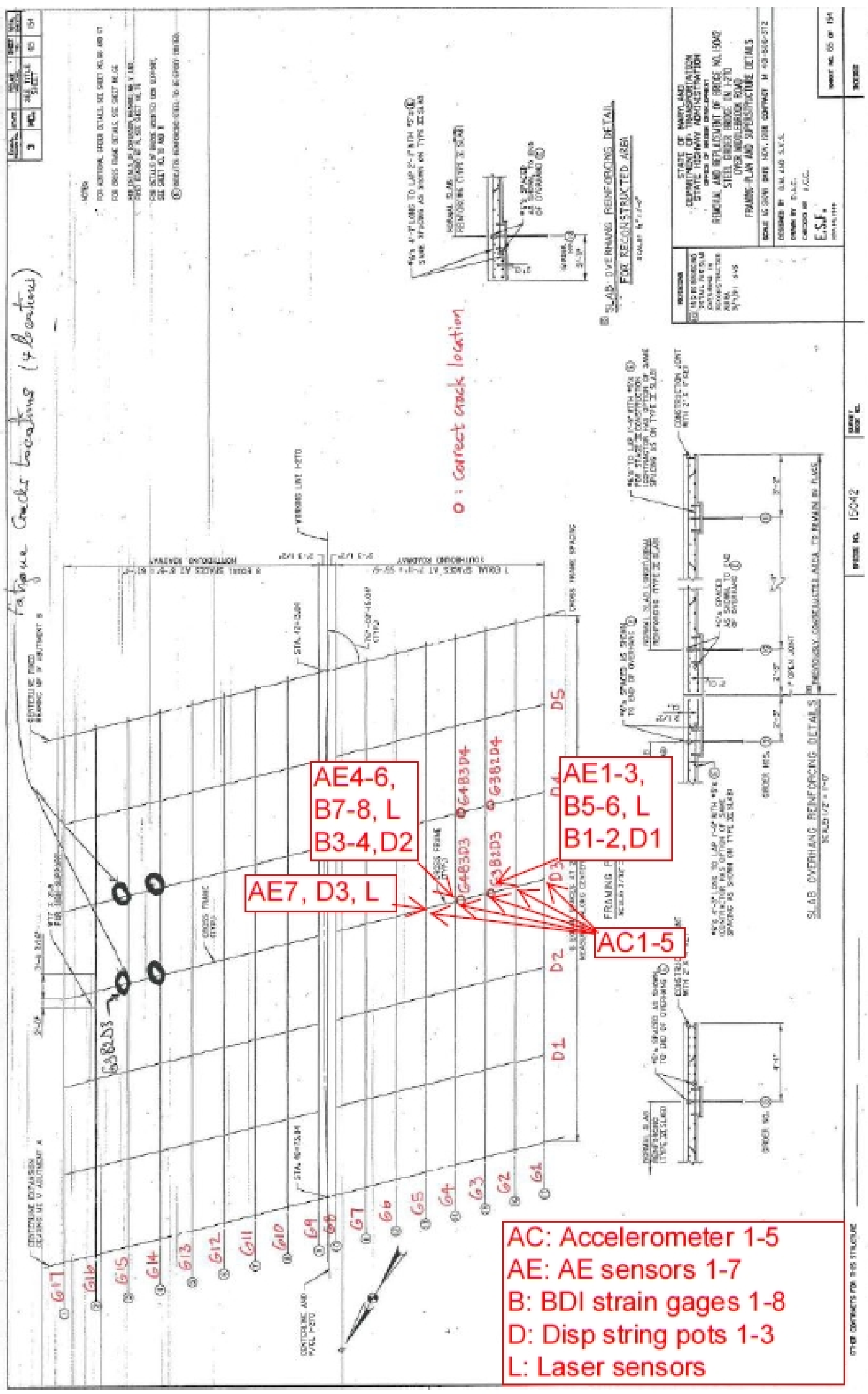

Figure 1 – Crack locations and sensor placement on the framing plan

In order to investigate the cause of cracks, global and local models were built. Details of those two models are described below.

A. Global Model

1. Modified global model

Modified finite element global model was generated for the bridge earlier. The modified global model contains the connection plates, and refined meshed around the hot spots for analysis. The modified model shown in Figures 2 and 3 has almost the same nature frequency as the former model. Its first natural frequency is calculated around 3.16 for a fixed-fixed boundary condition and 2.23 for a fixed-free boundary condition as reported earlier. After calibrating the model, the traffic loading can be added on and the analysis can be conducted.

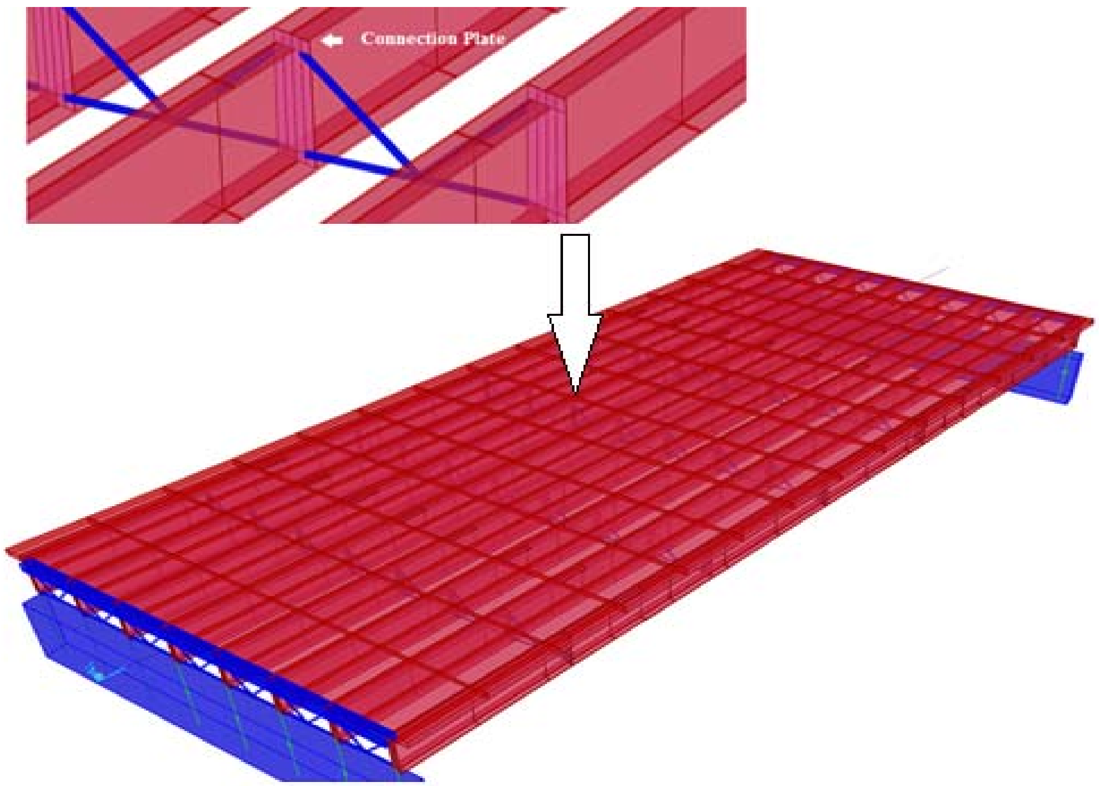

Figure 2 – Global Model with Connection Plates

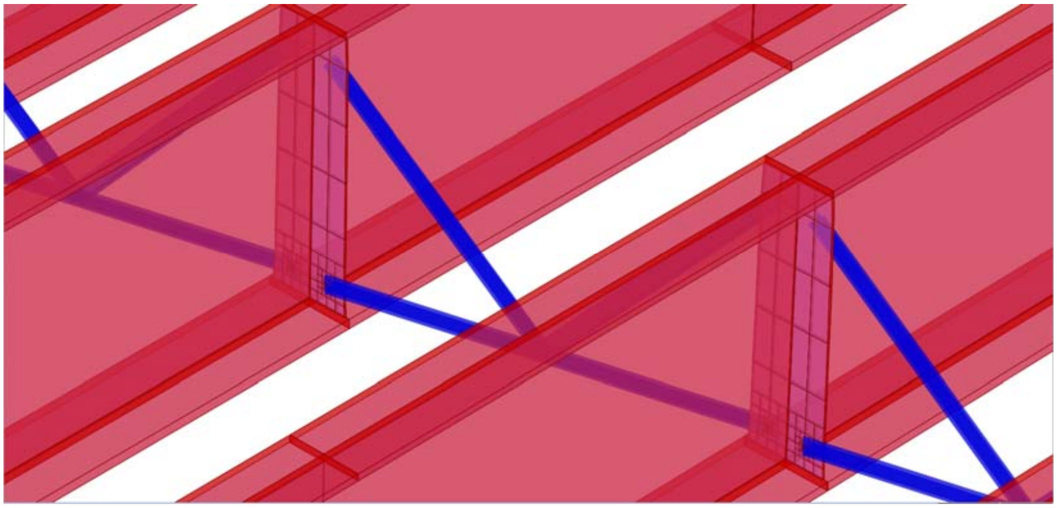

Figure 3 – Zoom-in View (Refined Meshed around the hot spot)

2. Results

(1)Displacement

Figure 4 shows the displacement time history of midpoints at the bottom flange for Girder 3 and Girder 4. The maximum differential displacement is 0.08 in under simulated traffic loading.

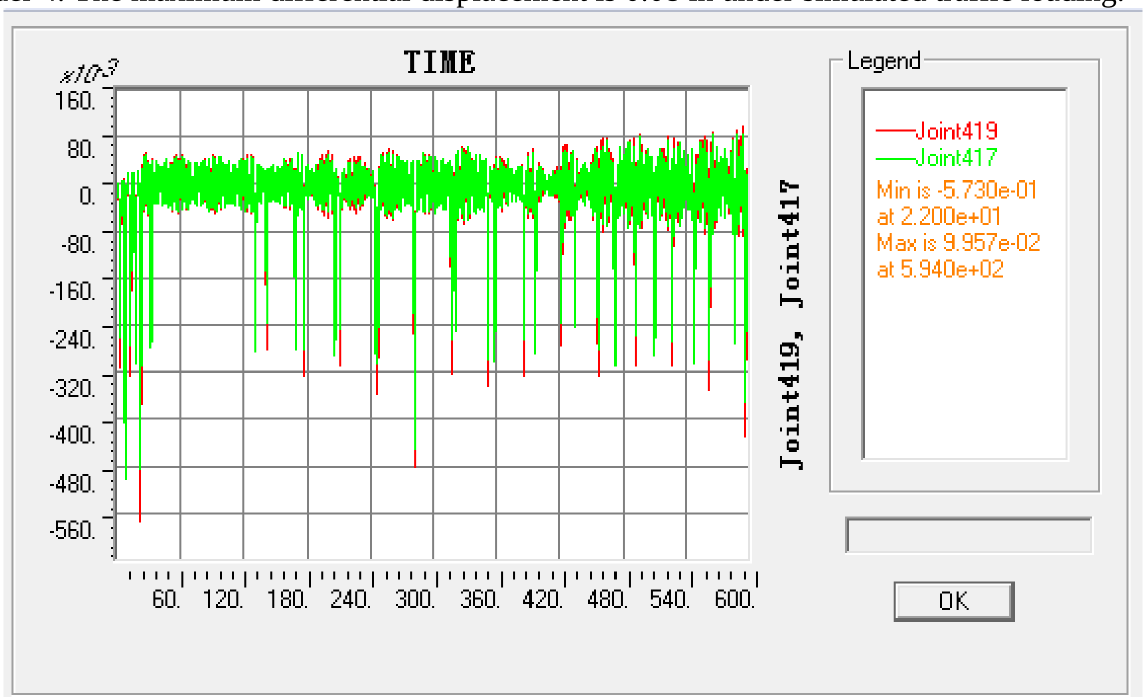

Figure 4-Midpoint displacements for G3(Joint 419) and G4(Joint417),unit in

(2)Stress

Check the hot spots where BDI strain transducers were placed. Figure 5 shows the time history curves of two hot spots of the connection plate, located at Girder 3 Diaphragm 3. Shell element 252 is on the G3crack side, and shell element 250 is on G3 uncrack side. Both of them are on the same face. The plot in Figure 6 represents that one side of the connection plate is under compression while the other is under tension. The maximum tension stress is 17.86ksi, and the maximum compression stress is 11.79ksi.

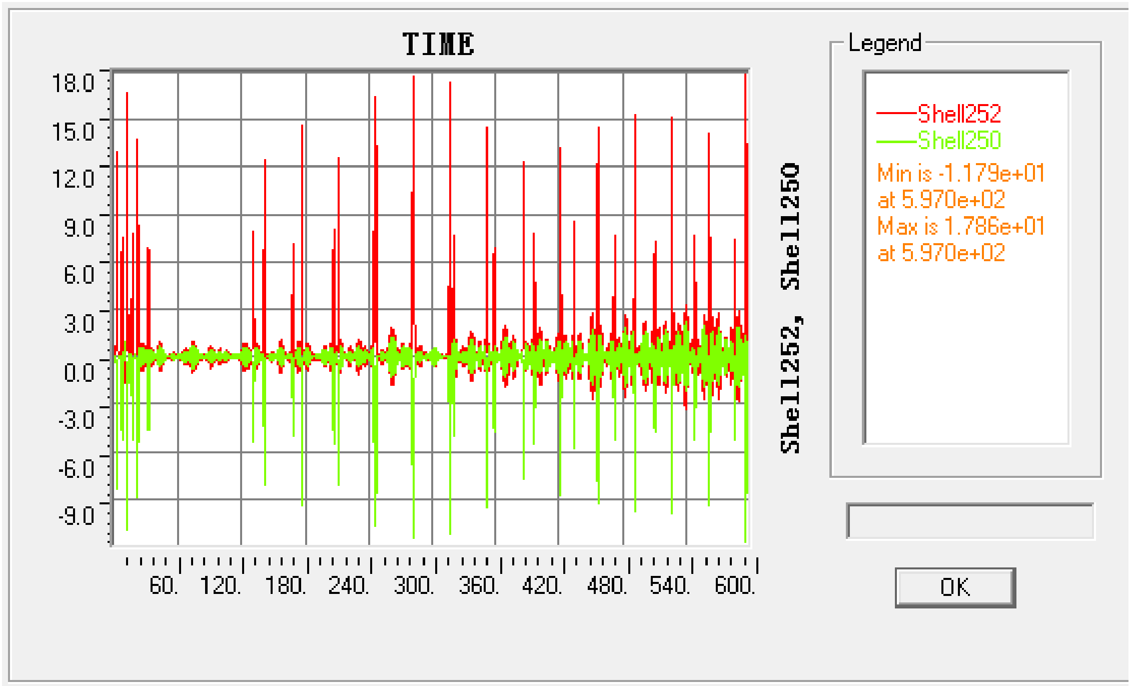

Figure 5-Stress of Hot Spot (Shell252-G3crack side, shell250-G3uncrack side) unit-ksi

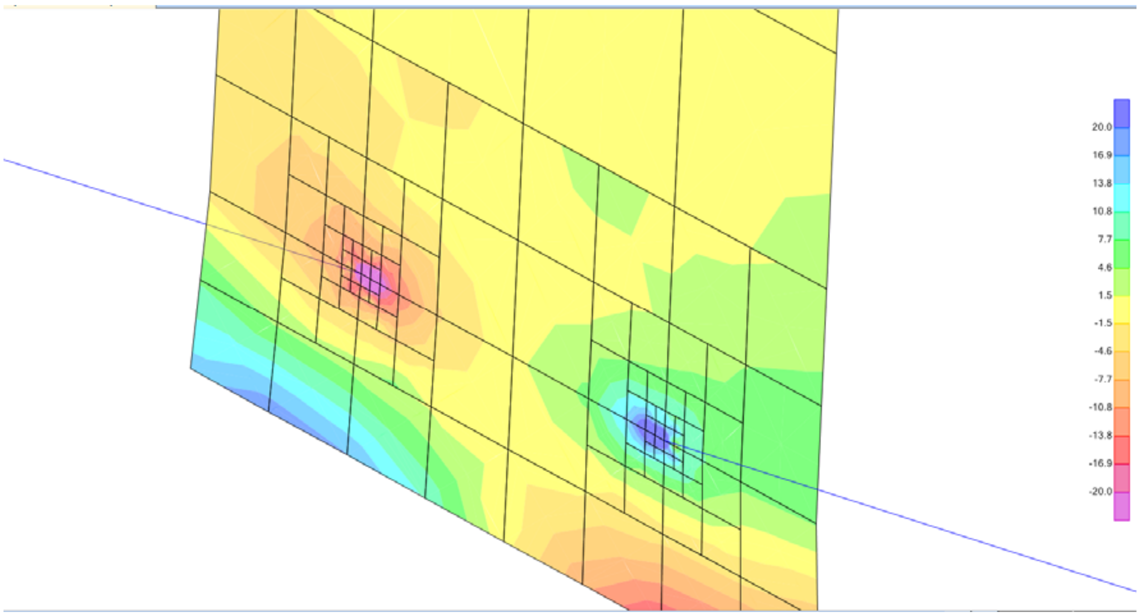

Figure 6-Stress Contour of Connection Plate (Girder 3 Diaphragm 3) at T=597second

Figure 7 shows the time history curves of two hot spots of the connection plate, located at Girder 4 Diaphragm 3. Shell element 316 is on the G3crack side, and shell element 328 is on G3 uncrack side. Both of them are on the same face. The plot in Figure 8 represents that one side of the connection plate is under compression while the other is under tension. The maximum tension stress is 21.45ksi, and the maximum compression stress is 9.622ksi.

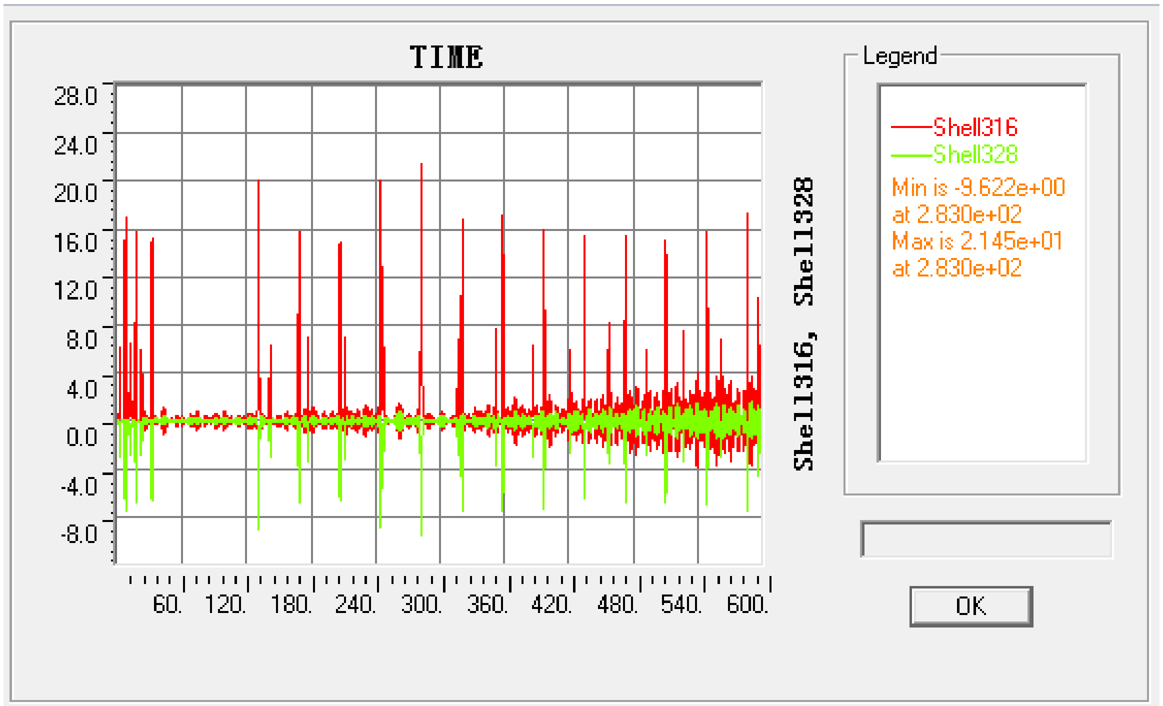

Figure 7-Stress of Hot Spot (Shell316-G4crack side, shell328-G4uncrack side) unit-ksi

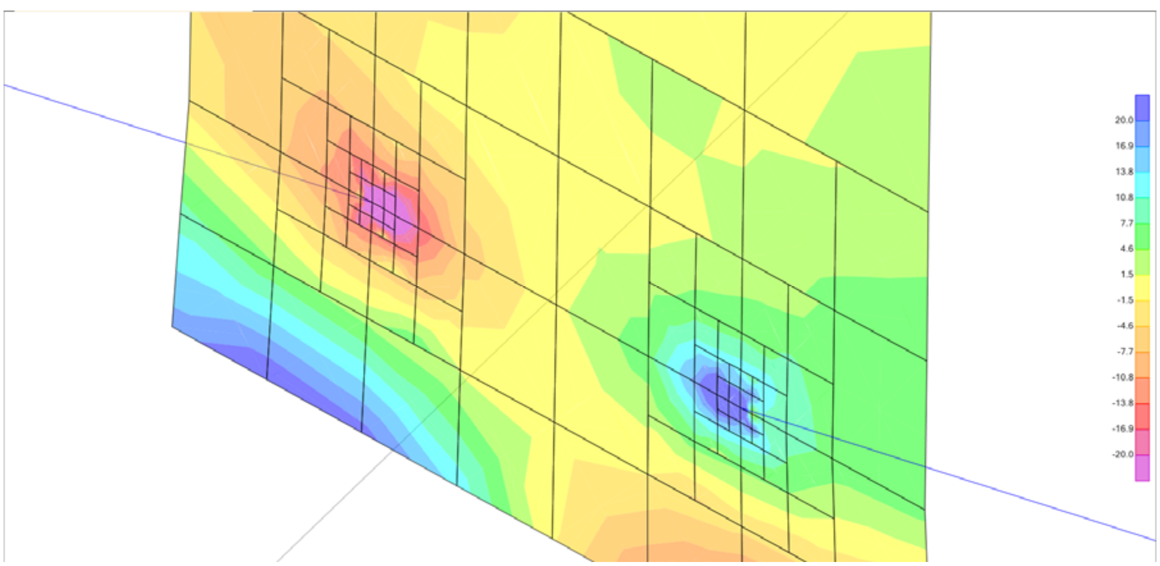

Figure 8-Stress Contour of Connection Plate (Girder 4 Diaphragm 3) at T=283 second

B. Local Model

Figure 9 shows the plan for typical K-type cross frame detail and Figure 10 shows the finite element local model in SAP 2000.

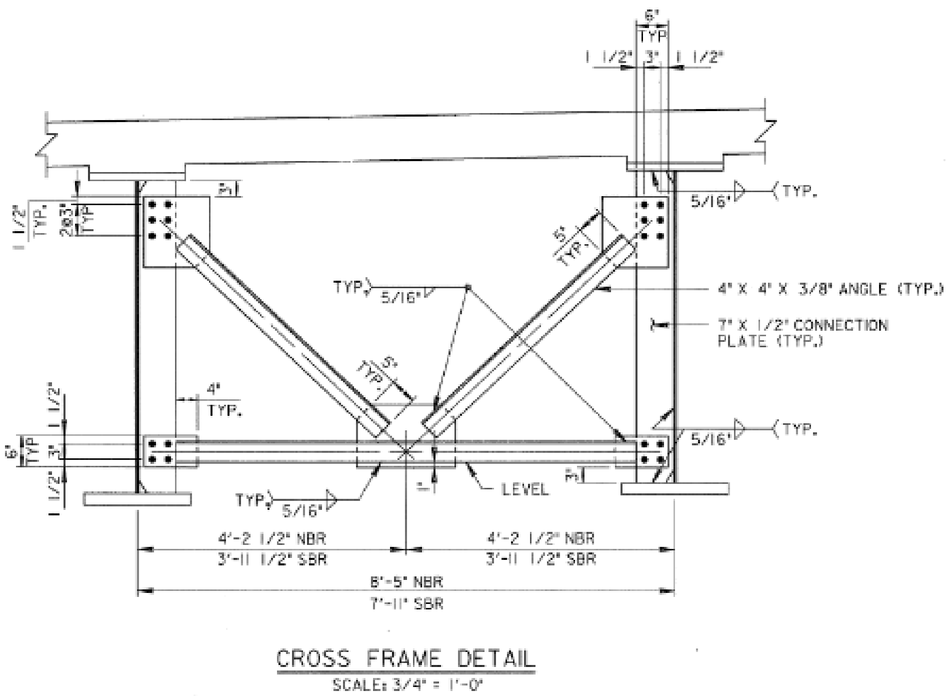

Figure 9 - Typical cross frame detail

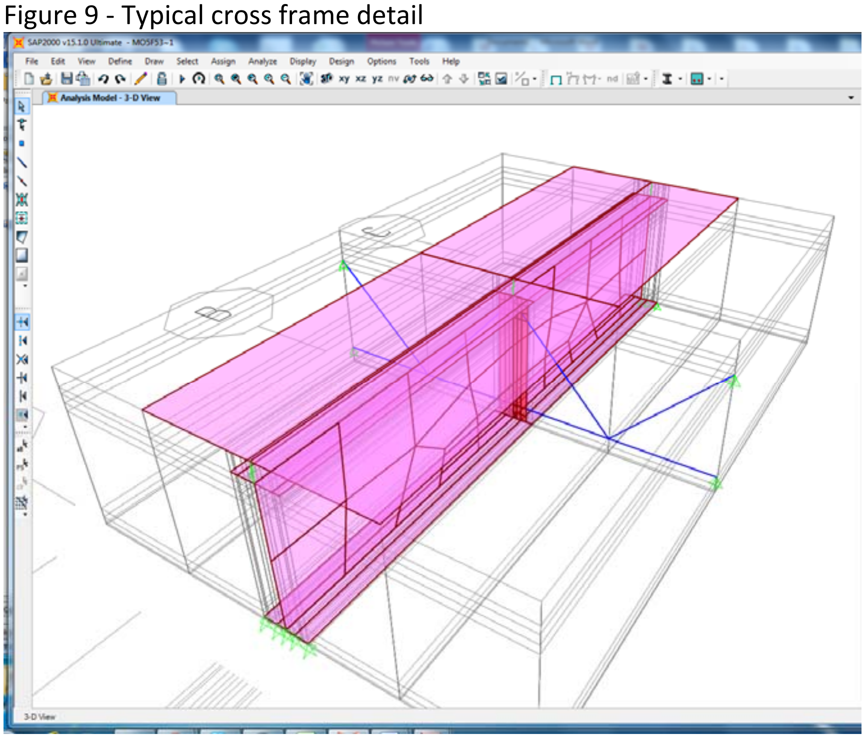

Figure 10 - Local model at mid span girder three

The model and its results are summarized below:

1) Local Model – portion of girder with K-type crossframes on both sides (Figure 10)
2) Boundary condition - pin supported (Figure 10)
3) Loading - 0.2in downward displacement on the left end and 0.4in upward displacement at the right end were applied (Figure 10)
4) Maximum stress around bottom chord and connection plate connection (Figure 11)
   -1.7ksi compressive stress on the left connection plate
   +4.07ksi tensile stress on the right connection plate

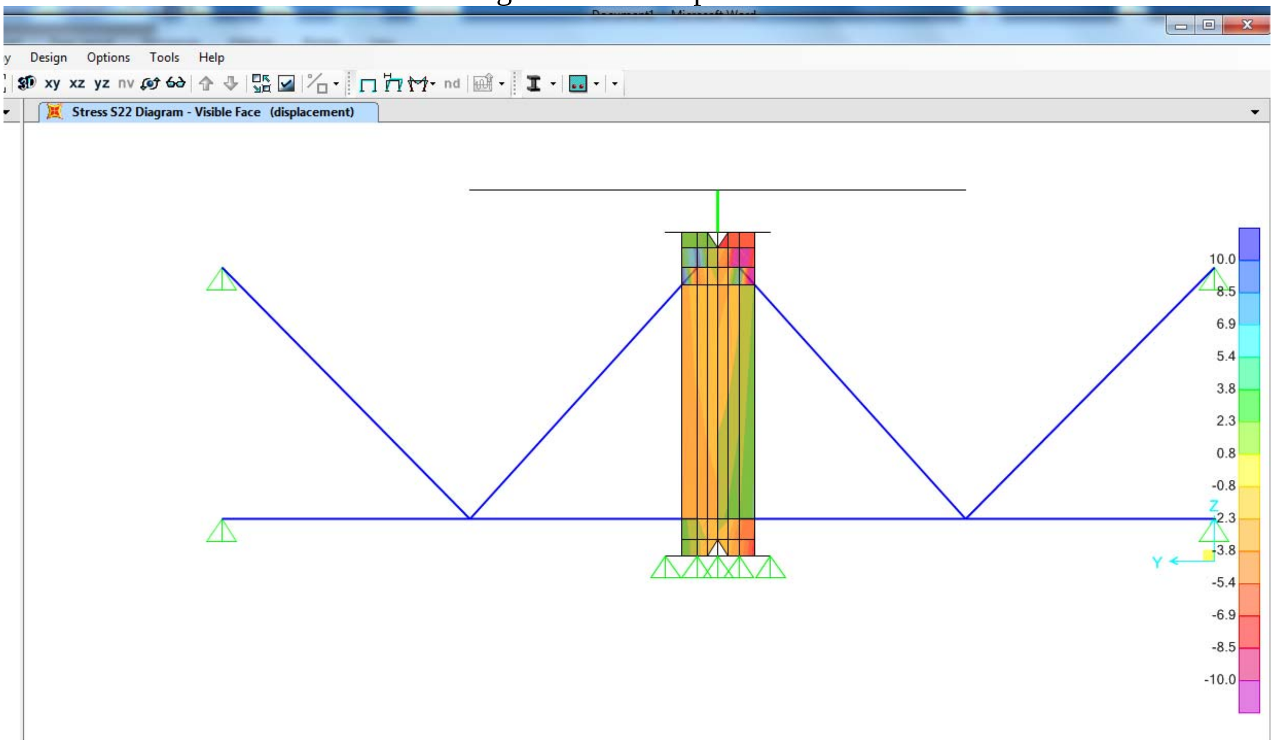

Figure 11 - Local model stress contour on connection plate

It can be concluded that among all types of cross-frames, X-type with top and bottom chords is the stiffest of all, then the K-type with top and bottom chords, then the X-type with bottom only and the flexible one is the K-type with bottom chord only. Differential displacement between girders will cause one diagonal in tension and one in compression. Since the working point of the diagonal is not at the junction of girder web and top flange plus no help from the top chord, one side of the connection plate will be under tension and one under compression. Measured 16.1 ksi in tension is not surprising with the flexibility of the cross-frame and the girder system (with up to 0.5" to 0.75" vertical deflections due to live load observed.)

Appendix E – NCST Report for NC Beaufort County Bridge

- Wireless accelerometer sensor and its performance test

Each single wireless sensor was tested on a shaker, which excited by a sinusoidal wave with a frequency of 15Hz. The acceleration time-history and the power spectral densities (PSD) of the test data are shown in Fig. 1. It can be seen from the figure that the peak of the PSD is the frequency of the driving signal, which demonstrates that the developed sensor can accurately recover the information of these data.

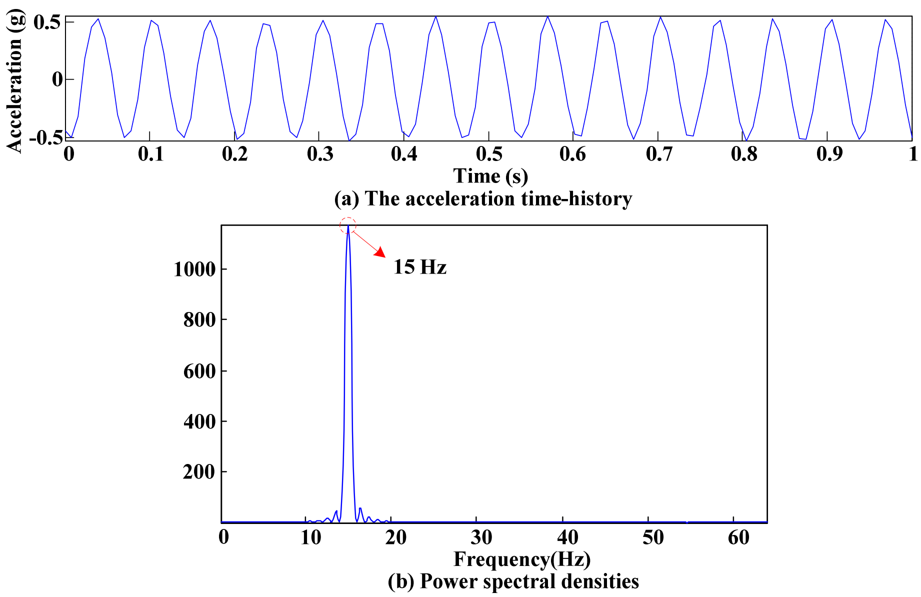

Fig. 1 Test results of the single sensor

- Performance tests of the whole WSN

The above test just demonstrated that every wireless sensor functioned well, however the information collected by a single sensor is rather simple for extracting the state of a structure. Thus a number of wireless sensors along the span of the structure were installed to collect structural dynamic information of the structure to be monitored. The WSN is composed of five sensors on a bridge in Lake Raleigh, shown Fig. 2, was installed to test the performances of this system, which include time synchronization, data acquisition and data transmission (point to point transmission). Fig. 3 is the acceleration time-history of sensor 3 acquired under two different scenarios: (a) one person continuously jumping on the bridge; and (b) one person running back and forth on the bridge. The PSD of these sensors under these different loading cases are drawn in Fig. 4. It can be seen from the figure that the natural resonance frequency (around 3.4 and 5 Hz) calculated by each sensor and the same sensor under different scenarios agreed well, which demonstrated that the WSN performed well and can be used for acquiring information from a structure. Fig. 5 shows the first two modal shapes of this small bridge.

Fig. 2 Sensor locations on the test bridge

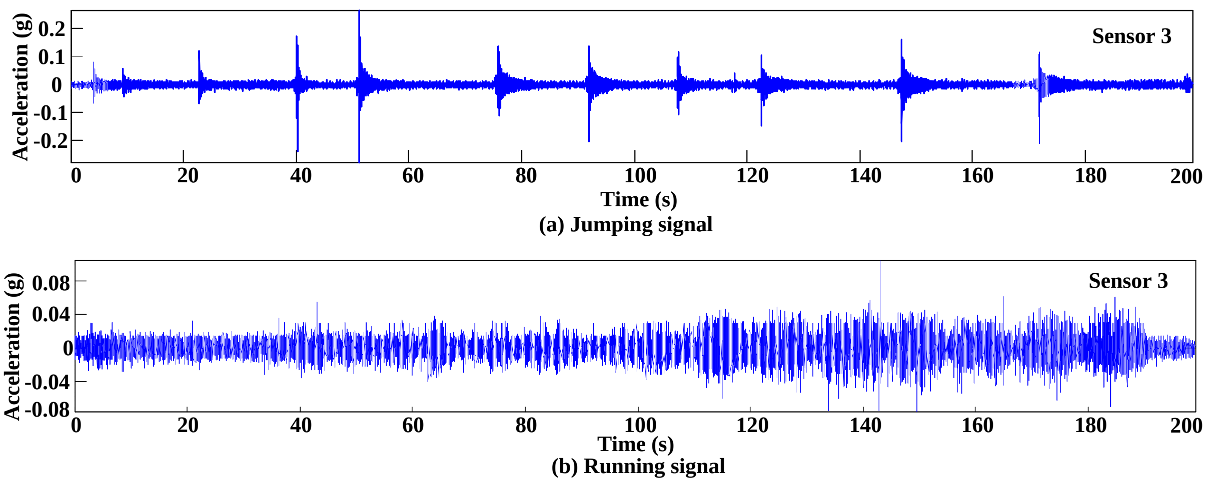

Fig. 3 The acceleration time history of sensor 3 under different cases

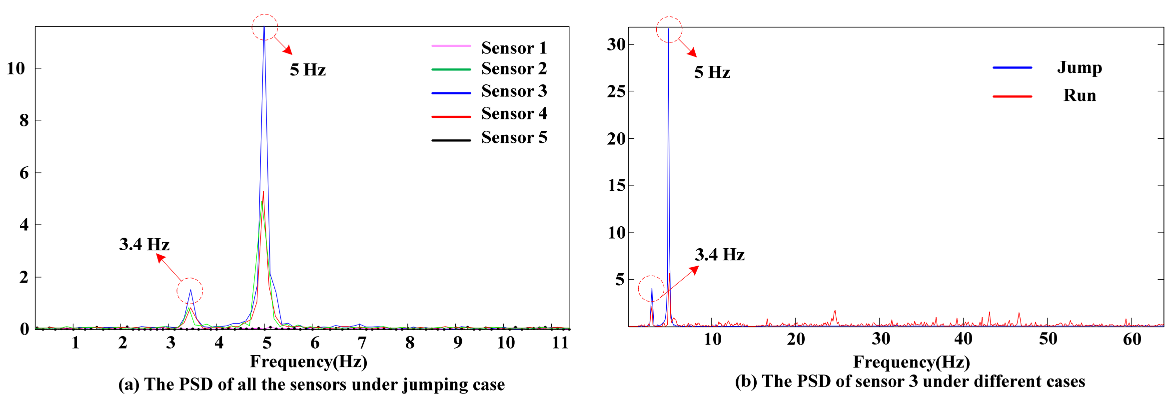

Fig. 4 The PSD of

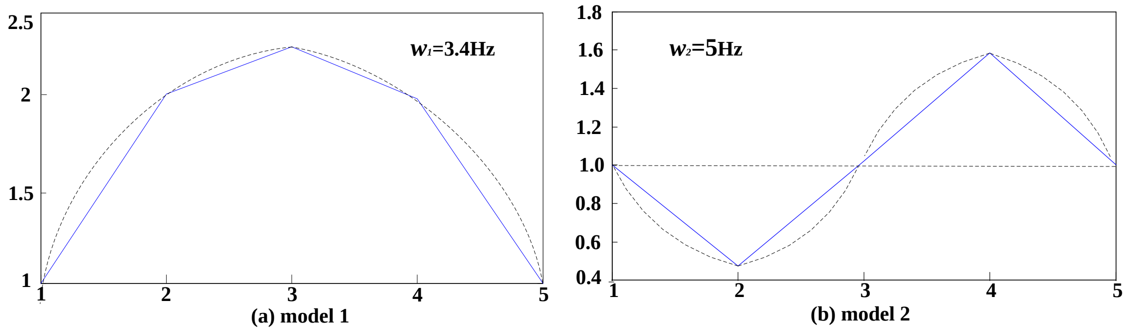

sensors

Fig. 5 The first two mode shapes

- Installment of Energy Harvesting System

A total of seven wireless sensors were deployed on the bridge and each equipped with an energy harvesting device located at where the sensor was installed. Each of this device collects both solar power and wind energy for supplying power to the sensor (seen in Fig. 6). These sensors are located at 1/2 span, a quarter of span and the support.

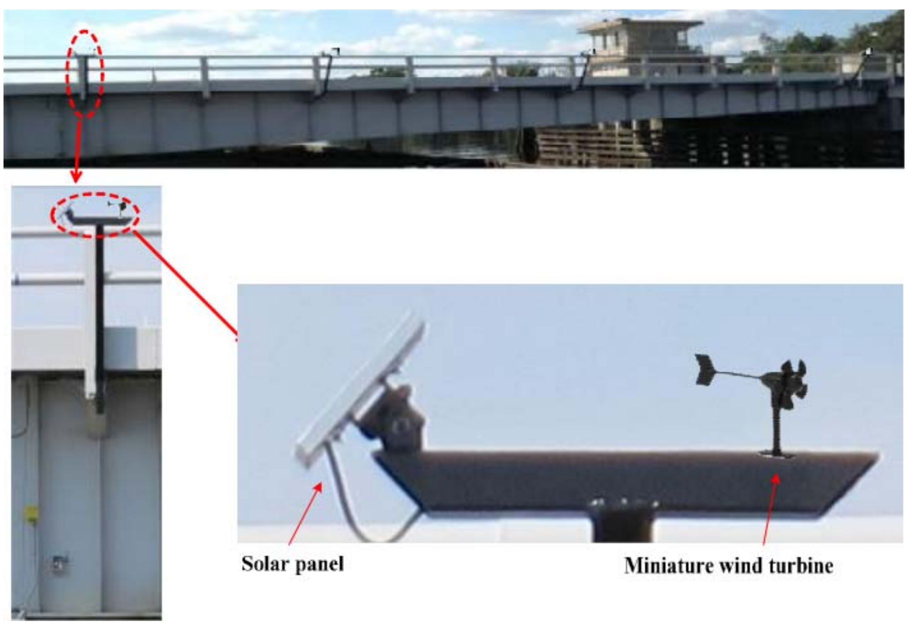

Fig. 6 Energy harvesting devices

- Installment of Base station

For the entire wireless sensor network, It is critical for the base station providing access to the WSN. The functions of the base station in the SHM system include: (1) sending commands to the wireless sensors, (2) reading and storing the transmitted data from the WSN, (3) processing received data and (4) transferring the data to the FTP server via internet. To achieve these functions, the base station is composed of a netbook running Windows XP OS, an uninterrupted power supply, a gateway node and an environmentally hardened enclosure, shown in Fig. 7.

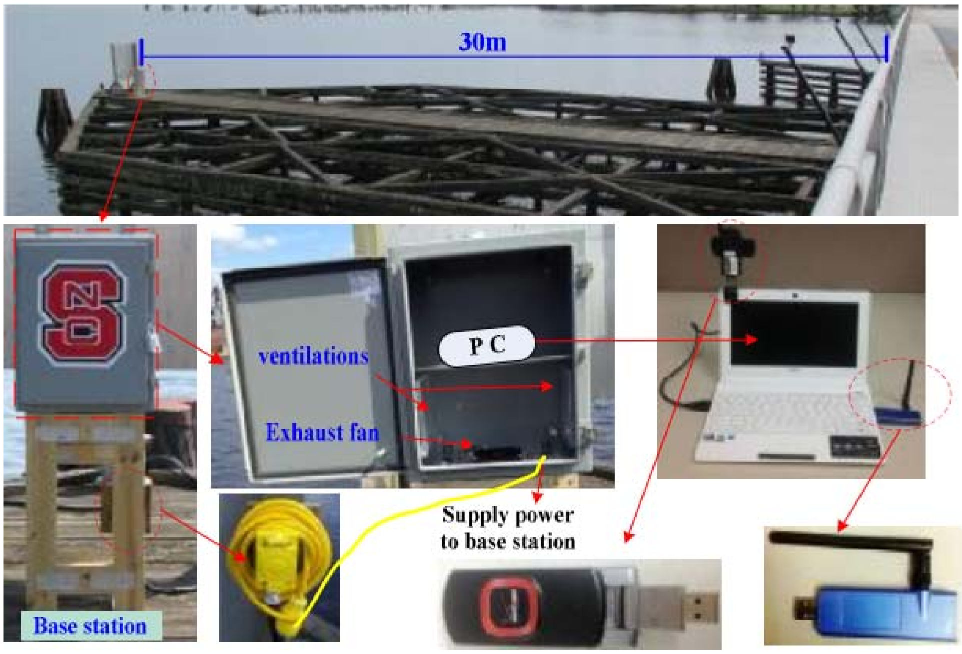

Fig. 7 Base station

A plan for maintaining long-term durability of the base station is proposed when it is exposed to environmental load such as sunlight, rain, snow, fog and harsh winds. To protect electric components from damage, waterproof socket was employed to provide power to the base station as shown in Fig. 7. In order to keep a fitness temperature inside the enclosure, some ventilations openings have anti-bug nets and rain-protection brackets, and the exhaust fan is connected to a temperature sensor inside the enclosure. The fan will automatically turn on when the temperature in the enclosure is over 35^{O}C. In addition, a high power external antenna is mounted to the enclosure and then connected to the gateway with an antenna extension cable. The 4G LTE network support by Verizon is used to transmit the data from base station to FTP server via internet.

- Finite element analysis of Beaufort #25 Bridge

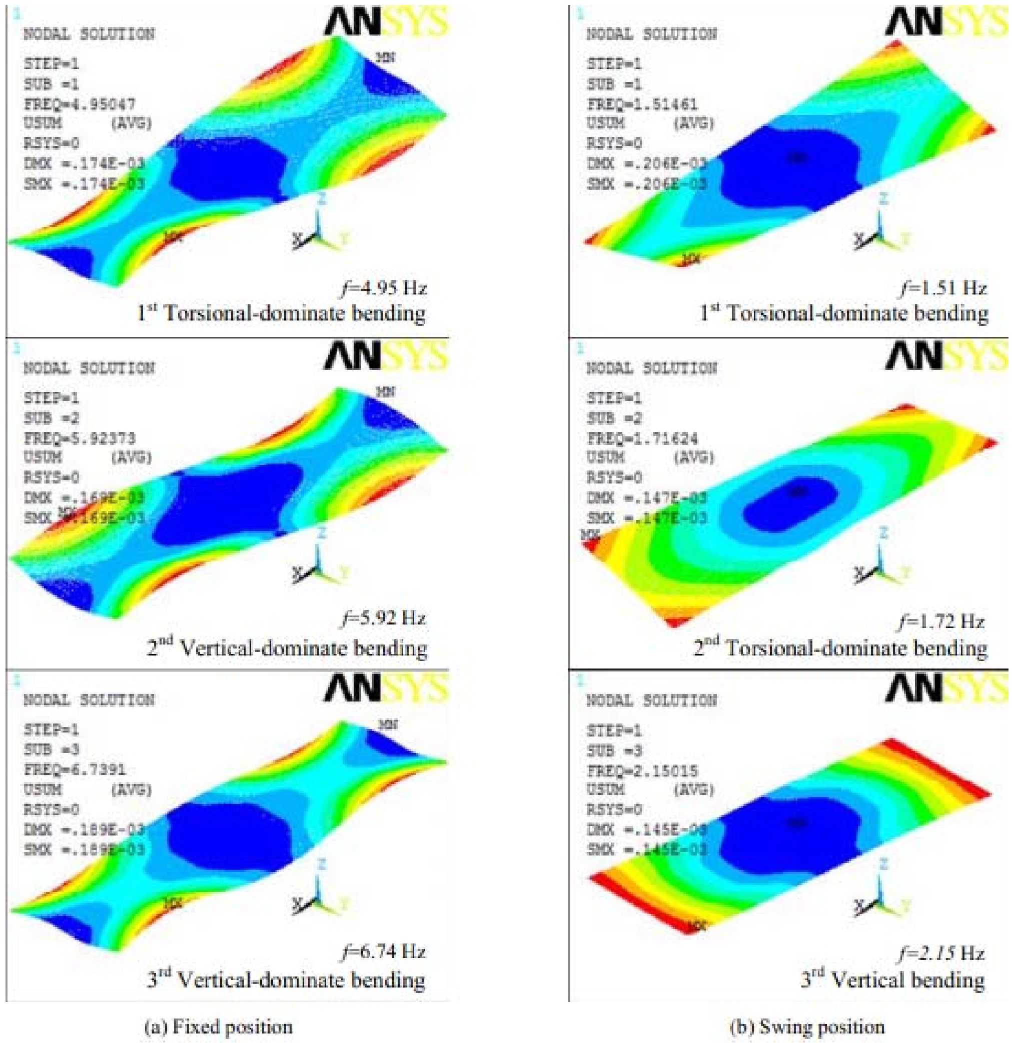

Fig. 8 The first three mode shapes from FE analysis

Table 1 Modal analysis results

Fixed Position		Swing Position	
1st (Torsional)	4.95 Hz	1st (Torsional)	1.51 Hz
2nd (Vertical)	5.92 Hz	2nd (Torsional)	1.72 Hz
3rd (Vertical)	6.74 Hz	3rd (Vertical)	2.15 Hz
4th (Vertical)	7.48 Hz	4th (Vertical)	2.51 Hz
5th (Lateral)	8.18 Hz	5th (Vertical)	2.58 Hz

The FE model of Beaufort #25 Bridge was built and analyzed. The first five modes are summarized in Table 1. Depending on the relative amplitudes of the model shapes, these modes can be classified into the three groups: the vertical-dominated modes, the lateral-dominated modes, and the torsional-dominated modes. The first three mode shapes are illustrated in Fig. 8.